Per. Mineral. (1999), *68*, 1, 13-42

PERIODICO di MINERALOGIA
established in 1930

An International Journal of
MINERALOGY, CRYSTALLOGRAPHY, GEOCHEMISTRY, ORE DEPOSITS, PETROLOGY, VOLCANOLOGY
and applied topics on *Environment, Archaeometry* and *Cultural Heritage*

Origin of glass and its relationships with phlogopite in mantle xenoliths from central Sardinia (Italy)

MICHELE LUSTRINO*, LEONE MELLUSO and VINCENZO MORRA

Dipartimento di Scienze della Terra, Università «Federico II», Via Mezzocannone, 8 I-80134 Napoli, Italy

Submitted November 1998 - Accepted April 1999

ABSTRACT. — Spinel-bearing lherzolite and harzburgite mantle xenoliths from central Sardinia (Italy) contain glassy patches with clinopyroxene and spinel relicts together with euhedral crystallites of olivine, clinopyroxene and spinel. Although texturally uniform, the glass may be chemically distinguished into two groups: the first type with low K_2O (mean 0.07 ± 0.05 wt%) and TiO_2 (mean 0.68 ± 0.12 wt%; LKT-type), and the second type with high K_2O (mean 2.51 ± 0.82 wt%) and TiO_2 (mean 3.14 ± 0.35 wt%; HKT-type). All glass compositions are quartz-normative. Rare phlogopite laths are enclosed in olivine or orthopyroxene crystals. The following mass balance equations have been obtained both for HKT- and LKT-type glasses:

$$6.9\,Cpx_{(1)}+0.6\,Sp_{(1)} \Rightarrow 3.5\,Cpx_{(2)}+0.6\,Sp_{(2)}+0.1\,Ol_{(2)}+1.0\,Glass \text{ (LKT)}$$

and

$$7.9\,Cpx_{(1)}+0.5\,Sp_{(1)}+0.7\,Phl_{(1)} \Rightarrow 3.8\,Cpx_{(2)}+0.6\,Sp_{(2)}+0.1\,Ol_{(2)}+1.0\,Glass \text{ (HKT)}$$

where the subscripts (1) and (2) represent primary (reactant) and secondary (product) phases, respectively. Clinopyroxene + spinel ± phlogopite are expected to have melted incongruently to yield olivine, clinopyroxene and spinel. This suggests that the glasses are not the product of metasomatic processes, but derive by decompression melting of mantle xenoliths, probably after the incorporation in the host lava. Other evidences of early stages of partial melting come from the relatively abundant spongy-textured clinopyroxene. Recent experimental studies (Raterron *et al.*, 1997) evidence the incongruent partial melting of clinopyroxene at mantle depth several hundreds degrees below its conventional solidus temperature. Metasomatic processes in the Sardinian lithospheric mantle account for the origin of phlogopite in the xenoliths.

* Corresponding author. Present address: Dipartimento di Scienze della Terra, Università degli Studi «La Sapienza», P.le A. Moro, 5 I-00185 Roma, Italy. e-mail: lustrino@uniroma.it

RIASSUNTO. — Xenoliti ultrafemici di mantello provenienti dalla Sardegna centrale sono caratterizzati da zone vetrose associate a relitti di clinopirosseno e spinello. All'interno di questi vetri si rinvengono cristalliti euedrali di clinopirosseno, olivina e spinello. I vetri possono essere distinti chimicamente in due gruppi: LKT (Low K_2O-Type), caratterizzati da bassi contenuti in K_2O (media 0.07 ± 0.05 wt%) e TiO_2 (media 0.68 ± 0.12 wt%) e HKT (High K_2O-Type), caratterizzati da elevato K_2O (media 2.51 ± 0.82 wt%) e TiO_2 (media 3.14 ± 0.35 wt%). Entrambi i tipi di vetri sono quarzo-normativi. Sono stati rinvenuti anche rari cristalli di flogopite inclusa nell'olivina e ortopirosseno. Equazioni di

bilancio di massa condotte sui vetri e sulle altre fasi mantelliche hanno evidenziato una possibile origine dei vetri da fusione incongruente di clinopirosseno e spinello (± flogopite) con la formazione di un fuso (vetri) più nuovi cristalliti di clinopirosseno, olivina e spinello. In questo modello, la flogopite entrerebbe come fase reagente solo nella genesi dei vetri HKT, mentre le composizioni dei vetri LKT sarebbero interamente tamponate da clinopirosseno e spinello. La fusione parziale incongruente del clinopirosseno e dello spinello potrebbero essere dovuti alla decompressione in seguito all'incorporazione degli xenoliti nella lava incassante. Recenti studi sperimentali (Raterron *et al.*, 1997) hanno evidenziato la fusione incongruente del clinopirosseno circa 200° al di sotto della normale temperatura di solidus del diopside, con la formazione di un fuso ricco in SiO_2 più cristalliti euedrali di olivina, clinopirosseno e spinello. Gli eventi metasomatici responsabili per la presenza della flogopite negli xenoliti ultrafemici della Sardegna non sono quindi responsabili e non sono collegati alla presenza dei vetri.

KEY WORDS: *Glass, phlogopite, mantle xenoliths, metasomatism, Sardinia.*

INTRODUCTION

Mantle xenoliths are often recorded from intraplate alkaline rocks, but they are rare in subduction zones. For example, mantle xenoliths have been found in intraplate alkaline rocks from the Cenozoic European Volcanic Province (CEVP) (French Massif Central (e.g. Werling and Altherr, 1997), the Rhine-Rhön area (e.g. Franz and Wirth, 1997), Eifel (e.g. Zinngrebe and Foley, 1995), Carpathian-Pannonian basin (e.g. Rosenbaum *et al.*, 1997), northern Italy (Lessini Mts., Siena and Coltorti, 1993), Sicily (Mt. Etna, Aurisicchio and Scribano, 1987; and Hyblean Mts., Tonarini *et al.*, 1996), and Sardinia (Beccaluva *et al.*, 1989; Siena and Coltorti, 1993).

In general, these xenoliths contain the typical four phases (olivine, orthopyroxene, clinopyroxene and a minor chromian spinel phase) plus additional «exotic» phases (e.g. amphibole, mica, apatite, ilmenite, sulfides, carbonates, glass; Yaxley *et al.*, 1991; Ionov *et al.*, 1994; Sen *et al.*, 1996; Draper and Green, 1997). The origin of these phases is currently debated and has been related to controversial causes (e.g. Yaxley *et al.*, 1997). However, it is commonly thought that they represent the consequence of metasomatic processes (Menzies and Hawkesworth, 1987).

Many models have attempted to reconcile the geochemical and petrographic characteristics of metasomatized mantle xenoliths. These models speculate on the physical nature of the metasomatic agents (fluid or melt), their geochemical characteristics (silicate or carbonatitic materials, H_2O/CO_2 ratio, etc.), the genetic relationship of these agents with the mantle xenolith and the host lava (e.g. metasomatism as cause or consequence of magmatic activity), and the relationships between glass and hydrous phases.

Within the last few years, much attention has been paid to the origin of the discrete glass occurring in mantle xenoliths (e.g. Draper and Green, 1997). The overall composition of this glass is extremely variable, ranging from virtually alkali-free to alkali-rich compositions (< 1 wt% to 15 wt% $Na_2O + K_2O$) and SiO_2-poor to SiO_2-rich (~40 wt% to up to ~70 wt% SiO_2; Draper and Green, 1997). Moreover, two types of glasses, texturally and geochemically distinct, were often found in the same xenolith (e.g. Sen *et al.*, 1996; Chazot *et al.*, 1996; Franz and Wirth, 1997).

Petrological and geochemical studies on mantle xenoliths from Sardinia have focused only on the northern and central-eastern sectors of the island (Pozzomaggiore, Mt. Arci, Orosei-Dorgali; Beccaluva *et al.*, 1989; Siena and Coltorti, 1993), where large and fresh xenoliths are relatively common. The present paper reports a new set of mantle xenoliths from central-southern (Zeppara Manna and Pitzu Mannu) and southeastern Sardinia (Rio Girone, fig. 1). New chemical data on ultramafic xenoliths are presented and the nature of glass from worldwide mantle xenoliths are reviewed.

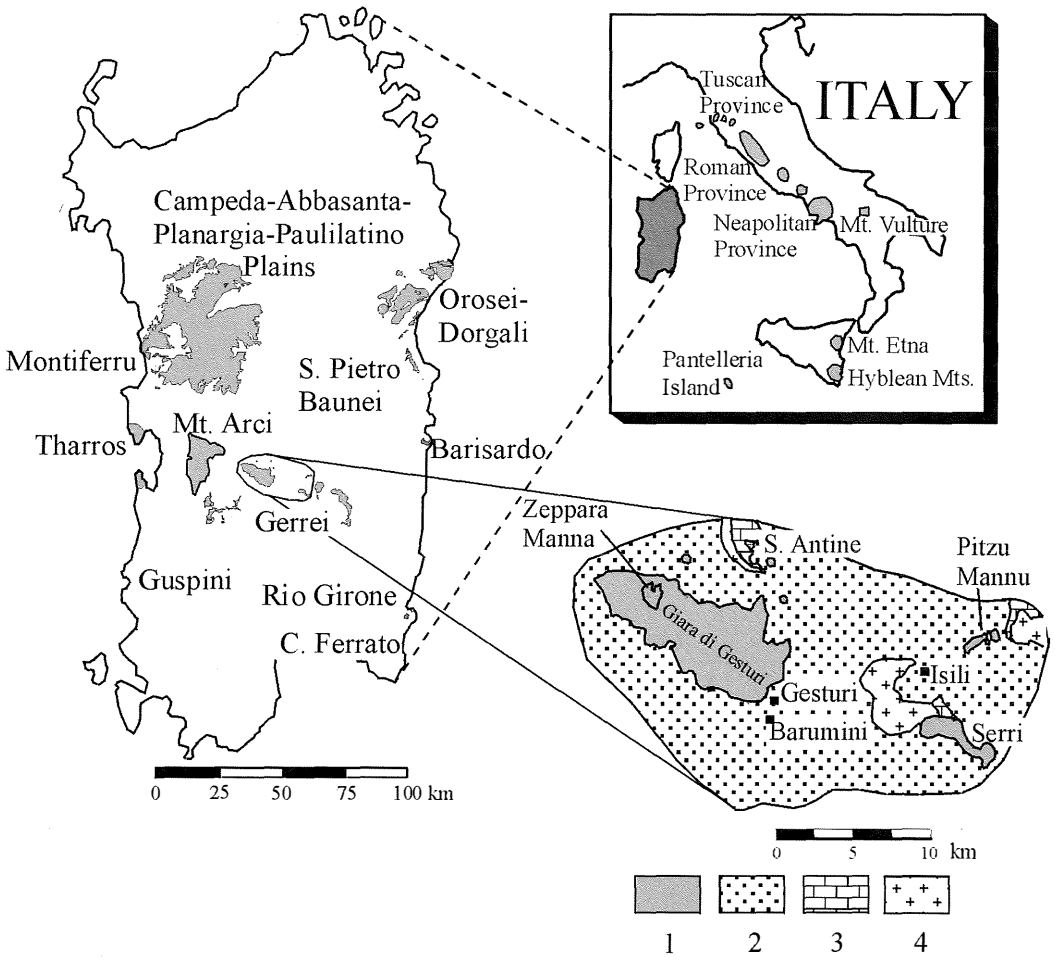

Fig. 1. – Simplified geological sketch map of the Gerrei Area (central Sardinia), modified from Lustrino (1999). 1 = Plio-Pleistocene volcanic rocks; 2 = Tertiary sediments; 3 = Permo-Mesozoic sedimentary and volcanic formations; 4 = Eruptive and metamorphic formations of the Paleozoic basement.

GEOLOGY AND SAMPLE LOCATIONS

The Plio-Pleistocene volcanic rocks from Sardinia cover about 2,000 km^2 (Lustrino, 1999). They occur as large volcanic complexes (Montiferro and Mt. Arci), as well as basaltic plateaux (Abbasanta-Paulilatino, Orosei-Dorgali and Gerrei), monogenetic volcanoes (Barisardo and Capo Frasca), cinder cones (Logudoro) and necks intruded in the Paleozoic basement (Rio Girone and Guspini). Tholeiitic to strongly alkaline rocks, together with mildly alkaline and transitional rocks have been found. The affinity of the alkaline rocks range from sodic to slightly potassic. This volcanic activity lasted 5.3 to 0.1 Ma after the final stage of the Oligo-Miocene orogenic activity (from ~32 to 15 Ma; Beccaluva *et al.*, 1985; Morra *et al.*, 1994, 1997).

Ultramafic inclusions are relatively common in Plio-Pleistocene alkaline rocks. These xenoliths span in composition from

TABLE 1

Major elements analyses (wt%) of representative host lavas and mantle xenoliths from Gerrei (central Sardinia) and Rio Girone (southeastern Sardinia). Avg. = average composition; St.D. = Standard deviation (±2σ). McD = average lithospheric mantle after McDonough, 1980; Jag79 = primordial mantle after Jagoutz et al., 1979.

	Host lavas			Zeppara Manna mantle xenoliths								L.M.	P.M.
	AB	Hw	Bsn	GG	Cr-Di	NOD1	NOD2	NOD3	NOD4	Avg.	St.D.	McD	Jag79
SiO_2	49.76	50.01	45.55	45.27	44.67	44.12	43.93	44.70	43.62	44.39	0.51	44.00	45.13
TiO_2	2.20	2.06	3.11	0.14	0.05	0.12	0.15	0.13	0.01	0.10	0.05	0.09	0.22
Al_2O_3	15.19	15.05	15.13	2.42	0.72	3.17	2.92	3.05	2.85	2.52	0.78	2.27	3.97
Fe_2O_{3t}	10.99	10.11	11.63	8.72	8.72	9.78	10.09	9.72	9.69	9.45	0.50	9.36	8.69
MnO	0.13	0.15	0.16	0.17	0.17	0.21	0.22	0.21	0.21	0.20	0.02	0.14	0.13
MgO	8.89	7.75	7.51	40.18	44.71	38.44	39.03	37.95	39.66	40.00	2.07	41.40	38.30
CaO	8.05	7.12	10.32	2.67	1.49	2.76	2.35	2.91	2.55	2.46	0.43	2.15	3.50
Na_2O	4.18	4.01	3.47	0.15	0.14	0.34	0.28	0.32	0.29	0.25	0.07	0.24	0.33
K_2O	1.79	2.65	2.22	0.01	0.01	0.01	0.01	0.01	0.01	0.01	0.00	0.01	0.03
P_2O_5	0.40	1.07	0.39	0.02	0.01	0.04	0.03	0.01	0.02	0.02	0.01	0.06	-
Mg#	0.65	0.63	0.59	0.89	0.90	0.88	0.87	0.87	0.88	0.88	0.01	0.89	0.89
V	186	178	254	47	42	66	57	66	63	57	9	56	77
Nd	n.d.	36	n.d.	8	8	14	11	11	9	10	2	2.67	-
Cr	335	258	139	2297	2233	2722	2546	2446	2453	2450	148	2690	-
Ba	1070	1224	702	n.d.	n.d.	29	29	20	22	25	4	33	6.9
Zn	96	113	93	59	65	62	62	61	62	62	2	65	50
Ni	167	187	52	1415	1432	1227	1198	1212	1343	1305	89	2160	2110
Rb	30	47	53	1	2	n.d.	2	3	2	2	1	1.9	0.81
Sr	820	904	884	10	10	13	13	11	7	11	2	49	28
Y	20	21	30	5	4	4	4	5	5	5	0	4.4	4.6
Zr	227	257	245	8	8	n.d.	9	n.d.	n.d.	8	0	21	11
Nb	38	44	77	1	1	3	2	3	4	2	1	4.8	0.9

harburgites/*cpx*-poor lherzolites to rare wehrlites and pyroxenites. Harzburgite-lherzolite xenoliths form about 75% of the total amount of xenoliths (Beccaluva *et al.*, 1989). The mantle xenoliths considered in this study were sampled in the small alkali basalt center of Zeppara Manna (ZM), located above the Giara di Gesturi tholeiitic plateau (Lustrino *et al.*, 1996; fig. 1), from a neck at Pitzu Mannu (MGL), and from Rio Girone (RG).

HOST LAVAS

The host lavas from Zeppara Manna and Pitzu Mannu are porphyritic basalts and hawaiites (Table 1) with olivine, plagioclase and clinopyroxene ± oxide phenocrysts in a fluidal and glass-bearing groundmass. Olivine ranges from Fo_{88} to Fo_{85}, plagioclase is labradorite (An_{60-54}) and pyroxene is Ti-rich augite (Wo_{46-43} En_{44-41} Fs_{14-12} TiO_2 up to 2.4 wt%). The Rio Girone sample is a sodic basanite, with mostly titanaugite phenocrysts (TiO_2 1.8-4.4 wt%) showing hourglass zoning, minor olivine (Fo_{77-75}) and magnetite. Microlites of plagioclase (An_{65-54}), analcime and anorthoclase are present in the groundmass. Sometimes, small (< 1 cm) quartz xenocrysts with reaction rims made up of minute clinopyroxenes, as well as very rare xenoliths of metamorphic rocks of lower crustal origin were

also found. The host lavas do not represent possible primary liquids because of their low Mg# and low Cr and Ni (< 0.65, <350 ppm and < 170 ppm, respectively), suggesting fractionation processes at mantle depths before xenolith trapping (Lustrino *et al.*, 1996).

PETROGRAPHY OF THE XENOLITHS

The mantle xenoliths from Zeppara Manna, Pitzu Mannu and Rio Girone are sp-bearing harzburgites and lherzolites (*ol* 48-88%, *opx* 7-28%, *cpx* 1-18%, *sp* 1.9-5.1%; Table 2). In some xenoliths from Zeppara Manna pale yellow to reddish interstitial glass (< 6%) and few grains of phlogopite (< 1%) have been found. The smallest xenoliths (1-5 cm in size, generally from Rio Girone) show sharp, angular contact with the host lava, whereas the largest (up to 10-15 cm across from Zeppara Manna) are rounded (fig. 2*a*). The contacts between xenoliths and host lava are generally sharp (fig. 2*b*), but in some cases resorption of enstatite grains (likely reacting with the silica-undersaturated host lava) produced an irregular shape of the xenolith. Sometimes, particularly in the Rio Girone xenoliths, growth of hourglass-zoned titaniferous clinopyroxene (probably due to crystallization near the cooler surface of the xenolith) was observed (fig. 2*c*). Green Cr-diopside veins, about 5 mm wide, sometimes cross-cut the Zeppara Manna xenoliths.

Two dominant textures were observed:

1) *Protogranular* (Mercier and Nicolas, 1975), with grains of olivine and orthopyroxene (the latter often with exolution lamellae of clinopyroxene; fig. 2*d*) up to 4 mm in size, with smaller clinopyroxene and spinel (~1 mm). Olivine is commonly characterized by kink banding, with polygonization and recrystallization of grains into larger aggregates. Olivine and orthopyroxene grains are equant and show curved and smoothed grain boundaries, sometimes abutting in triple point junctions. Clinopyroxene is present as small crystals close to orthopyroxene and olivine, as well as blebs along the rims of orthopyroxene without apparent reaction relationships.

2) *Pyrometamorphic* (Pike and Schwarzman, 1977), with spongy clinopyroxene and melt pockets. The latter are made up by a glassy matrix including clinopyroxene and spinel relicts, skeletal olivine and tiny quench microlites of clinopyroxene and, more rarely, feldspar. Glass is present in some *cpx*-poor lherzolite xenoliths from Zeppara Manna. Hereafter the phases unrelated to the glass are defined as «primary», in order to distinguish them from the quench products of the glass («secondary» phases).

TABLE 2

Modal compositions of Zeppara Manna mantle xenoliths obtained with point counter. Ol = olivine; Opx = orthopyroxene; Cpx = clinopyroxene; Sp = spinel; Phl = phlogopite; Gl = glass.

Xenolith	Ol	Opx	Cpx	Sp	Phl	Gl	Counts
ZM	60.0	29.8	6.5	2.7	0.6	0.3	3700
ZM1	47.9	28.3	18.3	3.0	tr	2.5	4000
ZM2	61.0	13.7	14.2	5.1	0.3	5.7	4000
Nod1	56.2	23.0	12.2	4.1	0.3	4.1	3800
GG1	88.3	7.0	2.8	1.9	-	-	3300
GG2A	71.1	19.6	5.7	3.7	-	-	3500
GG2B	66.6	19.4	10.2	3.8	-	-	3900
GG2D	67.0	21.2	7.5	4.2	-	-	3500
GG2E	74.3	20.9	1.2	3.6	-	-	1900
SA1	71.0	22.1	4.7	2.3	-	-	1300

WHOLE ROCK CHEMISTRY

A subset of mantle xenoliths (ZM) was chosen for major and trace element analyses (Table 1). SiO_2 (41.40-45.27 wt%), TiO_2 (0.01-0.15 wt%), Al_2O_3 (0.72-3.17 wt%) and MgO (37.95-44.71 wt%) have a wide range, while K_2O is always below detection limits (<0.01 wt%). The xenolith with Cr-diopside veins (Cr-Di) shows the highest MgO and

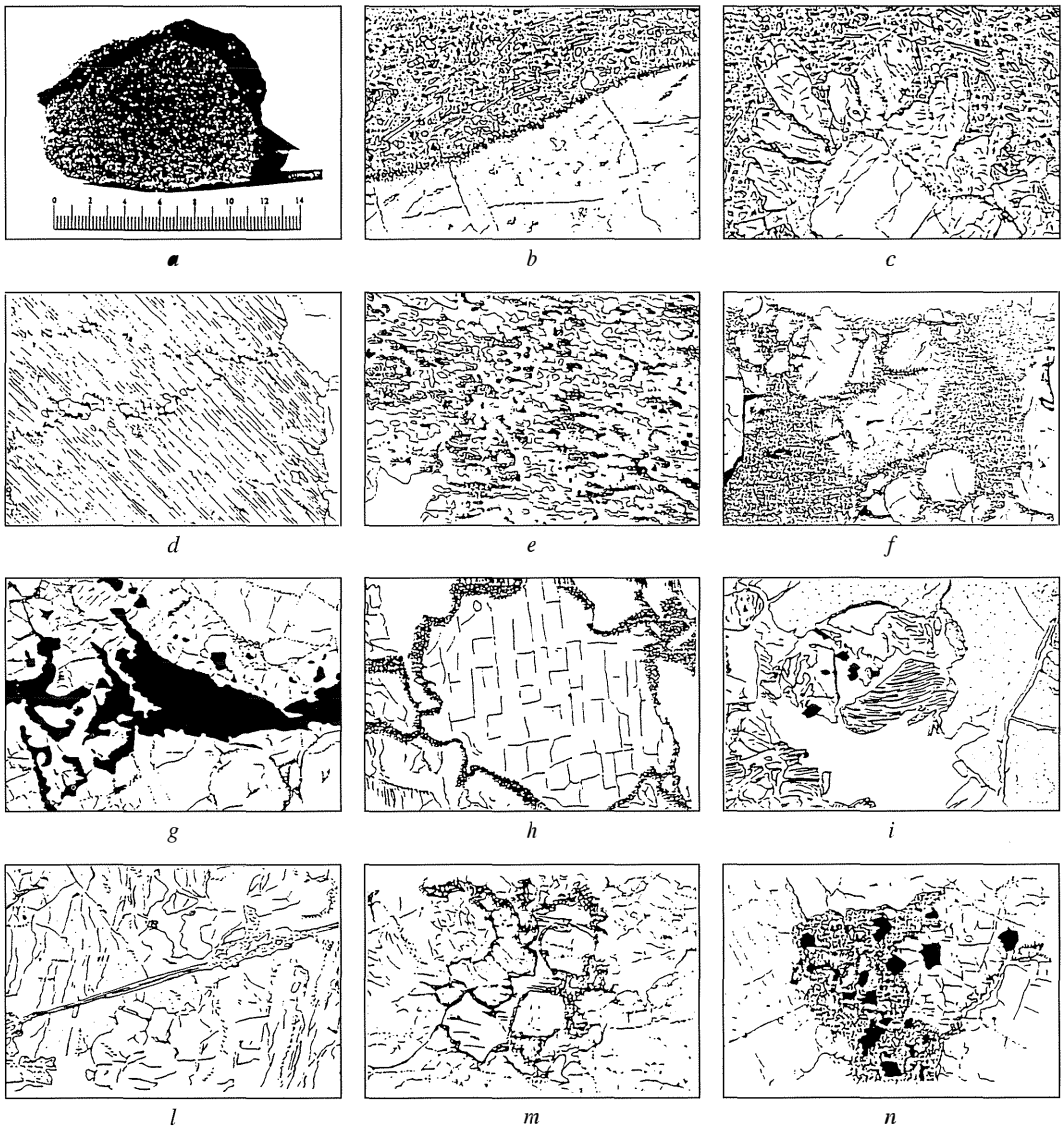

Fig. 2. – Pictures of mantle xenoliths from Gerrei area (central Sardinia) and from Rio Girone (southeastern Sardinia): *a)* = Zeppara Manna mantle xenolith of ab. 12 cm in width, cutted by a green Cr-diopside vein; *b)* = sharp mantle xenolith-host lava boundary from Rio Girone xenolith; *c)* = Ti-rich augite growth in host lava along Rio Girone xenolith boundary; *d)* = Exolution lamellae of clinopyroxene in larger orthopyroxene crystal in Pitzu Mannu mantle xenolith; *e)* = Spongy textured clinopyroxene in Zeppara Manna mantle xenolith; *f)* = Spongy textured clinopyroxene with a relict core from Zeppara Manna mantle xenolith; *g)* = Vermicular interstitial spinel between olivine and ortho- and clinopyroxene in Zeppara Manna mantle xenolith; *h)* = Reaction rim of picotite spinel in Zeppara Manna mantle xenolith; *i)* = Deformed laths of phlogopite close to olivine and orthopyroxene in Zeppara Manna mantle xenolith; *l)* = Phlogopite veinlet in olivine and orthopyroxene in Zeppara Manna mantle xenolith; *m)* = Interstitial phlogopite along olivine and orthopyroxene in Zeppara Manna mantle xenolith; *n)* = Pyrometamorphic glass including clinopyroxene and spinel relict. Olivine (top left) and orthopyroxene (bottom left) do not show reaction with the glass, differently from the clinopyroxene on the right of the picture.

TABLE 3

Selected microprobe analyses of olivine from mantle xenoliths from Gerrei and Rio Girone mantle xenoliths. Prim = primary; Sec = secondary (glass-related). Fo% = molar 100xMg/(Mg+Fe). Structural formulas calculated on the basis of 4 oxygens.

	RG3 Prim	RG3 Prim	GL22 Prim	GL22 Prim	ZM2 Prim	ZM2 Prim	ZM1 Prim	ZM1 Sec	ZM1 Sec	ZM1 Sec	ZM1 Sec
SiO_2	41.60	41.16	41.16	40.50	41.19	41.49	40.91	41.11	41.42	41.48	41.51
FeO	9.21	9.04	9.52	9.50	8.45	8.90	8.94	7.54	7.22	6.71	8.61
MnO	0.24	0.05	0.20	0.14	0.14	0.07	0.18	0.13	0.07	0.01	
MgO	48.30	48.08	49.70	50.42	48.24	48.29	47.62	48.65	50.54	49.68	49.12
CaO	0.14	0.13	0.03	0.02	0.15	0.16	0.11	0.16	0.15	0.30	0.10
NiO	0.55	0.57	nd	nd	0.64	0.66	0.60	0.26	nd	0.61	0.33
Sum	100.04	99.03	100.61	100.58	98.81	99.57	98.36	97.85	99.41	98.79	99.67
Si	1.017	1.015	1.001	0.986	1.016	1.017	1.016	1.024	1.009	1.020	1.018
Fe^{2+}	0.188	0.186	0.194	0.194	0.174	0.183	0.186	0.157	0.147	0.138	0.176
Mn	0.005	0.001	0.004	0.003	0.003	0.002	0.004	0.003	0.001	0.000	0.000
Mg	1.759	1.767	1.801	1.830	1.774	1.765	1.763	1.806	1.836	1.822	1.796
Ca	0.004	0.003	0.001	0.001	0.004	0.004	0.003	0.004	0.004	0.008	0.003
Ni	0.011	0.011	-	-	0.013	0.013	0.012	0.005	0.000	0.012	0.007
Sum	2.984	2.985	3.000	3.014	2.984	2.983	2.984	3.000	3.000	3.000	3.000
Fo %	90.3	90.5	90.3	90.4	91.1	90.6	90.5	92.0	92.6	93.0	91.1

lowest Al_2O_3, TiO_2, Fe_2O_{3t}, MnO, CaO and Na_2O. On the basis of mineralogy, modal proportions, mineral compositions, textures, rock types and chemical compositions, the ZM xenoliths belong to the group I (or Cr-diopside series) of Frey and Prinz (1978).

Compared to the primitive mantle estimate of Jagoutz *et al.* (1979) the ZM samples are slightly depleted in basalt components (Ti, Al, Ca, and alkalies), whereas, with respect to the lithospheric mantle of McDonough (1990), the xenoliths have broadly the same chemical composition, except for a slight enrichment in TiO_2.

MINERAL COMPOSITIONS

Olivine

Primary olivine has quite constant composition ($Fo_{91.5-89.3}$; Table 2), with high NiO (0.26-0.66 wt%) and low CaO (0.02-0.16 wt%) and MnO (0.01-0.24 wt%). Occasionally, higher CaO and lower FeO were observed respectively at the boundary with clinopyroxene and spinel, whereas, at the contact with the host lava, the forsterite content (Fo_{77-74}) overlaps with the values of olivine in the groundmass, suggesting Mg/Fe reaction exchange. Rare relicts of olivine partially enclosed in the glass are compositionally similar to the uncorroded olivine. The crystallites of olivine included in pyrometamorphic glass (secondary olivine) differ from primary olivine in their being euhedral and for their higher forsterite ($Fo_{93.0-91.0}$) and CaO (0.1.-0.30 wt%) and lower FeO (6.71-8.61 wt%), as generally reported for worldwide glass-related olivine (e.g. Girod *et al.*, 1981; Yaxley *et al.*, 1997). The higher CaO could be related to shallower depth of equilibration where these microlites possibly nucleated.

Orthopyroxene

Orthopyroxene is enstatite, often showing exsolution lamellae of clinopyroxene (fig. 2*d*). The range in Mg# (molar 100Mg/(Mg+Fe^{2+})) is narrow (91.6-89.5), overlapping the values of coexisting primary olivine (Table 4), with variable Cr# (molar 100Cr/(Cr+Al)) ranging from 22.6 to 4.5. At the contacts with phlogopite, enstatite shows high Al_2O_3 (up to 4.3 wt%), and TiO_2 (up to 0.4 wt%). Al_2O_3 in orthopyroxene from Rio Girone is constant (3.54-3.59 wt%), whereas samples from Zeppara Manna and Pitzu Mannu yielded Al_2O_3 negatively correlated with silica. Orthopyroxene was never found as quenched phase in the pyrometamorphic glass, and only very rarely as partially corroded relict phase in the melt pockets.

Clinopyroxene

Clinopyroxene occurs as: 1) small interstitial grains between larger olivine and orthopyroxene; 2) spongy-textured crystals; 3) relict and quenched microlite in

TABLE 4

Selected microprobe analyses of orthopyroxene from Gerrei and Rio Girone mantle xenoliths. Mg# = molar 100×Mg/(Mg+Fe^{2+}); Cr# = molar 100xCr/(Cr+Al). Structural formulas calculated on the basis of 6 oxygens and normalized to 4 cations. Fe^{2+} and Fe^{3+} according to Droop (1987).

	RG3	RG3	ZM-1	ZM1	ZM1	ZM2	ZM2	ZM2	MGL2	MGL22
SiO_2	54.81	53.85	55.31	57.48	56.40	55.31	54.36	54.99	55.06	55.03
TiO_2	0.17	0.01	0.25	0.01	0.05	0.15	0.42	0.01	0.10	0.03
Al_2O_3	3.57	3.59	3.05	1.84	1.93	2.84	4.35	2.76	3.92	3.66
FeO	6.25	6.48	6.38	7.20	5.49	5.65	6.26	6.02	5.98	5.73
MnO	0.05	0.10	0.19	0.19	0.25	0.04	0.13	0.20	0.15	0.18
MgO	33.42	33.61	32.96	34.54	33.38	33.96	32.69	33.74	33.05	33.97
CaO	0.63	0.59	1.07	0.30	1.71	0.59	0.87	0.64	1.31	0.88
Na_2O	0.16	0.29	0.31	0.01	0.03	0.32	0.27	0.30	0.03	0.04
Cr_2O_3	0.38	0.36	0.13	0.07	0.84	0.36	0.47	0.52	0.34	0.26
Sum	99.44	98.88	99.65	101.65	100.08	99.22	99.82	99.18	99.94	99.78
Si	1.898	1.871	1.915	1.953	1.948	1.913	1.880	1.906	1.901	1.898
Ti	0.004	0.000	0.007	0.000	0.001	0.004	0.011	0.000	0.003	0.001
Al	0.146	0.147	0.124	0.074	0.078	0.116	0.177	0.113	0.160	0.149
Fe^{3+}	0.048	0.121	0.050	0.018	0.002	0.063	0.046	0.079	0.025	0.055
Fe^{2+}	0.133	0.068	0.135	0.186	0.156	0.100	0.135	0.096	0.147	0.110
Mn	0.002	0.003	0.006	0.006	0.007	0.001	0.004	0.006	0.004	0.005
Mg	1.725	1.740	1.701	1.749	1.718	1.750	1.685	1.743	1.701	1.746
Ca	0.023	0.022	0.040	0.011	0.063	0.022	0.032	0.024	0.049	0.033
Na	0.011	0.020	0.021	0.001	0.002	0.022	0.018	0.020	0.002	0.003
Cr	0.010	0.010	0.004	0.002	0.023	0.010	0.013	0.014	0.009	0.002
Sum	4.000	4.000	4.000	4.000	4.000	4.000	4.001	4.001	4.001	4.000
Wo	1.2	1.1	2.1	0.5	3.2	1.1	1.7	1.2	2.5	1.7
En	89.4	89.1	88.0	88.8	88.2	90.4	88.6	89.5	88.3	89.6
Fs	9.4	9.8	9.9	10.7	8.5	8.5	9.7	9.3	9.2	8.7
Mg#	90.5	90.2	90.2	89.5	91.6	91.5	90.3	90.9	90.8	91.4
Cr#	6.7	6.3	2.8	2.6	22.6	7.8	6.8	11.2	5.5	4.5

TABLE 5

Selected microprobe analyses of clinopyroxene from Gerrei and Rio Girone mantle xenoliths. Prim = primary (interstitial); Spon (spongy); Sec = secondary (glass-related). Mg# = molar 100×Mg/(Mg+Fe^{2+}); Cr# = molar 100×Cr/(Cr+Al). Structural formulas calculated on the basis of 6 oxygens. Fe^{2+} and Fe^{3+} according to Droop (1987).

	RG4b Prim	RG4b Prim	ZM-2 Prim	ZM-2 Prim	ZM2 Prim	ZM-1 Prim	ZM-1 Prim	ZM-1 Prim	ZM-1 Prim	MGL22 Prim	Nod1 Prim	ZM-1 Spon	ZM1 Spon	Nod1 Sec	Nod1 Sec	Nod1 Sec
SiO_2	53.62	53.74	52.66	49.32	50.64	52.27	53.07	49.42	53.20	52.45	53.27	52.64	50.06	51.17	53.61	54.04
TiO_2	0.39	0.39	0.72	1.73	1.19	0.38	0.32	0.70	0.28	0.36	0.31	0.26	0.49	0.30	0.09	0.15
Al_2O_3	4.06	4.07	5.79	5.79	6.13	3.66	2.98	7.15	3.65	5.85	3.79	3.73	5.66	5.21	2.83	2.10
FeO_t	3.91	3.91	4.34	3.33	3.13	3.28	2.55	3.49	2.67	2.24	3.19	2.74	3.23	3.36	2.51	2.47
MnO	0.22	0.22	0.08	0.01	0.00	0.01	0.01	0.12	0.12	0.06	0.00	0.01	0.06	0.00	0.09	0.06
MgO	16.46	16.50	19.39	15.77	16.44	18.73	18.39	15.82	18.53	15.46	17.99	17.69	16.31	16.57	18.69	19.45
CaO	19.13	19.18	15.23	21.95	20.02	20.08	21.20	21.09	21.61	21.27	21.54	21.33	21.54	22.03	21.33	20.43
Na_2O	1.37	1.37	1.10	0.49	0.90	0.61	0.30	0.49	0.21	1.28	0.29	0.34	0.38	0.24	0.26	0.27
Cr_2O_3	0.54	0.54	0.58	1.25	1.46	0.51	1.15	1.12	0.21	0.93	0.76	1.34	1.41	0.93	1.12	1.16
Sum	99.70	99.92	99.89	99.64	99.91	99.53	99.97	99.40	100.48	99.90	101.14	100.08	99.13	99.82	100.51	100.12
Si	1.945	1.944	1.889	1.807	1.837	1.890	1.920	1.807	1.910	1.897	1.908	1.906	1.836	1.863	1.927	1.946
Ti	0.011	0.011	0.019	0.048	0.032	0.010	0.009	0.019	0.008	0.010	0.008	0.007	0.013	0.008	0.002	0.004
Al	0.174	0.174	0.245	0.250	0.262	0.156	0.127	0.308	0.154	0.249	0.160	0.159	0.245	0.224	0.120	0.089
Fe^{3+}	0.000	0.000	0.000	0.040	0.019	0.072	0.005	0.043	0.019	0.000	0.006	0.000	0.044	0.024	0.008	0.000
Fe^{2+}	0.119	0.118	0.130	0.062	0.076	0.028	0.072	0.064	0.062	0.068	0.090	0.083	0.055	0.078	0.067	0.075
Mn	0.007	0.007	0.002	0.000	0.000	0.000	0.000	0.004	0.004	0.002	0.000	0.000	0.002	0.000	0.003	0.002
Mg	0.890	0.890	1.036	0.861	0.889	1.009	0.991	0.862	0.992	0.834	0.960	0.955	0.891	0.899	1.001	1.044
Ca	0.743	0.744	0.585	0.862	0.778	0.778	0.822	0.826	0.831	0.824	0.827	0.828	0.846	0.859	0.822	0.789
Na	0.096	0.096	0.077	0.035	0.063	0.043	0.021	0.035	0.015	0.090	0.020	0.024	0.027	0.017	0.018	0.019
Cr	0.016	0.015	0.016	0.036	0.042	0.015	0.033	0.032	0.006	0.027	0.022	0.038	0.041	0.027	0.032	0.033
Sum	3.999	3.998	4.000	4.000	4.000	4.000	4.000	4.000	4.000	4.000	4.000	4.000	4.000	4.000	4.000	4.000
Wo	42.3	42.3	33.4	47.2	44.2	41.2	43.5	45.9	43.6	47.7	43.9	44.4	46.0	46.2	43.2	41.3
En	50.6	50.6	59.0	47.2	50.5	53.5	52.4	47.9	52.0	48.3	51.0	51.2	48.5	48.3	52.7	54.7
Fs	7.1	7.1	7.6	5.6	5.4	5.3	4.1	6.2	4.4	4.0	5.1	4.5	5.5	5.5	4.1	4.0
Mg#	88.2	88.3	88.8	89.4	90.3	91.0	92.8	89.0	92.5	92.5	91.0	92.0	89.8	89.8	92.8	93.2
Cr#	8.2	8.2	6.3	12.6	13.7	8.5	20.6	9.5	3.7	9.6	11.9	19.4	14.3	10.7	20.9	26.9

TABLE 6

Selected microprobe analyses of spinel from Gerrei and Rio Girone mantle xenoliths. Prim = primary (interstitial); Sec = secondary (glass-related). Mg# = molar 100×Mg/(Mg+Fe^{2+}); Cr# = molar 100×Cr/(Cr+Al). Structural formulas calculated on the basis of 32 oxygens. Fe^{2+} and Fe^{3+} according to Droop (1987).

	RG3 Prim	RG4-b Prim	ZM1 Prim	ZM1 Prim	ZM1 Prim	ZM1 Prim	MGL22 Prim	MGL22 Prim	ZM2 Prim	ZM2 Prim	Nod1 Prim	ZM2 Sec	ZM2 Sec	ZM2 Sec	ZM2 Sec
TiO_2	0.10	0.16	0.14	0.16	0.38	0.21	0.01	0.13	0.20	0.69	0.17	0.75	0.95	1.33	0.79
Al_2O_3	49.96	45.93	54.89	44.61	18.78	39.66	53.49	53.23	45.49	38.34	44.22	37.22	35.87	37.24	38.27
FeO_t	14.15	14.80	13.22	11.44	17.84	16.71	14.28	13.93	16.18	18.71	16.92	17.46	19.41	19.08	16.85
MnO	0.31	0.32	0.06	0.10	0.22	0.18	0.12	0.14	0.18	0.14	0.11	0.30	0.34	0.27	0.01
MgO	19.59	16.72	20.03	19.97	13.21	17.92	19.16	19.19	19.17	17.23	18.04	18.52	17.14	16.98	19.17
Cr_2O_3	14.83	16.30	11.07	21.57	45.45	24.17	14.43	14.99	17.63	23.38	18.01	23.15	23.72	22.90	24.40
Sum	98.94	94.23	99.41	97.85	95.88	98.85	101.49	101.61	98.85	98.49	97.64	97.56	97.44	97.80	99.49
Ti	0.016	0.028	0.022	0.026	0.074	0.035	0.002	0.020	0.033	0.118	0.028	0.128	0.164	0.230	0.132
Al	12.622	12.409	13.561	11.561	5.704	10.501	13.152	13.088	11.704	10.268	11.625	10.011	9.775	10.083	10.056
Fe^{3+}	0.822	0.576	0.556	0.631	0.878	1.115	0.462	0.396	1.166	1.271	1.123	1.519	1.522	1.273	1.349
Fe^{2+}	1.714	2.260	1.761	1.472	2.966	2.023	2.029	2.033	1.787	2.284	2.031	1.813	2.230	2.392	1.792
Mn	0.056	0.062	0.011	0.019	0.048	0.034	0.021	0.025	0.033	0.027	0.022	0.058	0.067	0.053	0.002
Mg	6.257	5.711	6.255	6.542	5.072	5.998	5.955	5.965	6.235	5.833	5.996	6.295	5.905	5.812	6.368
Cr	2.513	2.954	1.834	3.749	9.259	4.292	2.380	2.472	3.042	4.200	3.176	4.176	4.336	4.159	4.300
Sum	24.000	24.000	24.000	24.000	24.000	24.000	24.000	24.000	24.000	24.000	24.000	24.000	24.000	24.000	24.000
Mg#	77.9	71.1	77.9	81.4	62.7	74.5	74.4	74.3	77.4	71.6	74.5	77.1	72.0	70.4	78.0
Cr#	16.6	19.2	11.9	24.5	61.9	29.0	15.3	15.9	20.6	29.0	21.5	29.4	30.7	29.2	30.0

pyrometamorphic glass. Spongy-textured and relict clinopyroxene may indicate incipient partial melting of the xenoliths, as suggested by Pike and Schwartzman (1977). Clinopyroxene straddle the field of diopside and endiopside, with only small variation in FeO (Wo_{42-49} En_{43-53} Fs_{4-8}). Representative clinopyroxene compositions are given in Table 5. With respect to the coexisting olivine and orthopyroxene, wider Mg# and Cr# variations (92.8-88.2 and 20.6-3.7, respectively) were observed. As noted for olivine, euhedral microlites in glasses show higher Mg# up to 93.3. The spongy pyroxene (fig. 2*e*) shows low TiO_2 (0.26-0.32 wt%) and Al_2O_3 (2.9-3.8 wt%), and highest Cr_2O_3 (1.15-1.34 wt%). Clinopyroxene from the Cr-diopside veins has low CaO and the highest Na_2O.

Spinel

Spinel shows wide textural and chemical variations (fig. 2*g-h*, Table 6). It is present as: 1) black to reddish brown grains (up to 4 mm) with holly leaf or vermicular crystal habit in triple point junctions or included in pyroxene crystals; 2) small octhaedra associated with spongy clinopyroxene; 3) associated with glass both as relict phase and euhedral crystallite. Spinel ranges from chromiferous (Cr_2O_3 45.5 wt%; Al_2O_3 18.8 wt%), FeO-rich, to aluminous (Cr_2O_3 11.1 wt%; Al_2O_3 54.9 wt%), MgO-rich. Cr# ranges from 61.9 to 11.9, while Mg# vary from 81.5 to 62.8; these two parameters do not show any clear correlation. Spinel octhaedra associated with spongy clinopyroxene are interpreted as a newly formed phase subsequent to the incongruent melting of clinopyroxene into Cr-poor liquid and Cr-rich phase (spinel). Both «amorphus phase» and spinel octhaedra in the spongy clinopyroxene relict are too small to be analyzed.

Phlogopite

High-Ti phlogopite (TiO_2 3.22-4.72 wt%; Table 7) occurs in or between orthopyroxene

TABLE 7

Microprobe analyses of phlogopite from Zeppara Manna xenoliths. Av.H. = average of seven analyses of mica from host lava (Lustrino, 1999).

	ZM1					ZM2				Av. H.
SiO_2	37.75	37.61	37.89	37.58	38.29	37.25	37.59	38.18	38.03	40.87
TiO_2	3.47	3.44	3.72	3.22	3.47	4.26	4.17	4.64	4.66	5.406
Al_2O_3	16.64	16.34	15.99	16.01	17.56	15.97	16.09	16.72	16.41	11.42
Cr_2O_3	1.15	0.95	1.18	0.97	0.95	0.62	0.52	0.69	0.70	0.067
MnO	0.06	0.11	0.01	0.01	0.06	0.07	0.01	0.01	0.01	0.093
FeO	4.87	4.47	4.78	4.37	4.88	4.88	4.70	4.65	4.65	6.125
MgO	20.88	20.62	20.55	20.65	21.05	20.57	20.34	20.77	20.80	21.57
CaO	0.15	0.14	0.07	0.27	0.05	0.13	0.14	0.05	0.08	0.086
K_2O	9.18	9.25	8.72	8.50	8.97	8.98	9.24	8.81	8.80	9.589
Na_2O	0.55	0.58	0.88	0.77	0.43	0.84	0.55	0.94	0.76	0.738
BaO	0.24	0.29	0.33	0.41	0.36	0.52	0.47	0.57	0.64	0.42
F	0.37	0.96	0.35	0.22	n.d.	0.20	0.37	n.d.	n.d.	5.688
Cl	0.07	n.d.	n.d.	0.08	n.d.	0.06	0.06	n.d.	n.d.	0.107
Mg#	88.42	89.16	88.46	89.4	88.49	88.26	88.53	88.84	88.86	86.26

TABLE 8

Microprobe analyses and CIPW norm of pyrometamorphic glass from Zeppara Manna xenoliths. HKT = high K_2O-TiO_2 glasses; LKT = low K_2O-TiO_2 glasses. St.D. = Standard deviation at 2σ confidence. Mg# = (molar 100×Mg/(Mg+Fe)), assuming a Fe^{3+}/Fe^{2+} ratio = 0.15. R&al. 97 = Raterron et al., 1997.

	LKT GLASSES																Mean	St.D.	R&al. 97	
SiO_2	57.53	57.01	56.41	56.74	51.55	57.94	57.52	54.17	54.83	54.07	55.00	56.78	56.85	56.01	54.43	54.07	55.68	1.68	57.5	56.8
TiO_2	0.60	0.76	0.53	0.46	0.59	0.58	0.64	0.69	0.71	0.78	0.80	0.54	0.72	0.90	0.87	0.76	0.68	0.12	n.d.	n.d.
Al_2O_3	18.67	19.23	18.04	18.84	19.19	19.31	18.75	18.49	18.31	18.48	18.12	18.65	23.09	20.42	18.00	18.20	18.99	1.21	22.3	24.7
FeO_t	5.59	5.28	6.69	4.99	7.66	5.41	5.31	4.55	4.80	4.70	4.24	5.10	2.21	4.24	4.61	5.53	5.06	1.13	2.1	2.5
MnO	0.06	0.10	-	0.20	0.06	-	0.12	0.11	-	0.07	0.11	0.12	0.01	0.06	0.10	0.07	0.09	0.04	n.d.	0.1
MgO	5.17	5.31	4.98	5.32	5.70	4.11	4.82	5.14	5.05	5.07	5.00	5.03	0.91	3.31	6.35	6.83	4.88	1.28	7.6	4.3
CaO	10.98	10.74	10.89	11.03	13.55	8.74	9.62	12.47	12.17	12.69	12.13	10.39	11.04	10.68	12.07	12.64	11.36	1.21	7.2	10.8
Na_2O	1.57	1.84	2.26	1.42	0.88	2.87	2.21	1.93	2.06	2.38	2.16	2.33	2.07	2.01	1.59	1.49	1.94	0.46	3.2	0.6
K_2O	0.11	0.11	0.14	0.08	0.06	0.13	0.13	0.04	0.03	0.01	0.01	0.12	0.03	0.01	0.01	0.04	0.07	0.05	n.d.	n.d.
Cr_2O_3	-	0.18	0.08	0.05	0.11	-	-	-	0.06	0.12	0.07	0.08	-	-	-	-	0.09	0.04	0.1	-
F	0.14	0.05	0.13	0.08	0.24	0.05	-	-	0.03	-	-	-	-	-	-	-	0.10	0.07	n.d.	n.d.
Sum	100.41	100.59	100.18	99.24	99.58	99.14	99.12	97.66	98.09	98.38	97.64	99.12	96.93	97.64	98.03	99.63	98.84	1.07	100.0	99.8
Na_2O+K_2O	1.68	1.94	2.40	1.50	0.94	3.00	2.34	1.97	2.08	2.39	2.17	2.44	2.10	2.02	1.60	1.53	2.01	0.47		
Mg#	0.62	0.64	0.57	0.66	0.57	0.58	0.62	0.67	0.65	0.66	0.68	0.64	0.42	0.58	0.71	0.69	0.62	0.07		
CIPW Norm, assuming $Fe_2O_3/FeO = 0.15$																				
Q	18.07	16.75	14.61	17.72	9.26	18.08	18.05	13.23	14.04	11.69	14.51	15.98	22.76	18.86	13.71	11.40	15.55	3.29		
C	0.00	0.00	0.00	0.00	0.00	0.10	0.00	0.00	0.00	0.00	0.00	0.00	0.73	0.00	0.00	0.00	0.05	0.18		
or	9.30	10.84	13.33	8.37	5.22	16.98	13.08	11.41	12.16	14.03	12.76	13.74	12.23	11.88	9.40	8.80	11.47	2.70		
ab	0.93	0.89	1.21	0.71	0.51	1.07	1.07	0.30	0.22	0.12	0.12	0.97	0.25	0.08	0.08	0.34	0.56	0.40		
an	45.79	46.57	41.91	46.84	49.49	43.36	44.06	44.58	43.75	43.34	43.00	43.51	54.77	49.74	44.37	45.08	45.63	3.18		
ne	0.00	0.00	0.00	0.00	0.00	0.00	0.00	0.00	0.00	0.00	0.00	0.00	0.00	0.00	0.00	0.00	0.00	0.00		
di	7.05	5.44	9.94	6.40	14.54	0.00	2.96	13.98	13.43	15.84	13.85	6.52	0.00	2.64	12.45	14.21	8.70	5.32		
hy	16.99	17.48	16.74	17.27	17.73	17.43	17.72	11.95	12.14	10.89	11.05	16.39	4.43	11.97	15.54	17.37	14.57	3.66		
ol	0.00	0.00	0.00	0.00	0.00	0.00	0.00	0.00	0.00	0.00	0.00	0.00	0.00	0.00	0.00	0.00	0.00	0.00		
mt	1.07	1.01	1.28	0.96	1.47	1.03	1.02	0.87	0.92	0.90	0.81	0.98	0.42	0.81	0.88	1.06	0.97	0.22		
il	1.14	1.44	1.00	0.87	1.12	1.10	1.22	1.31	1.35	1.48	1.51	1.02	1.37	1.71	1.65	1.44	1.30	0.23		

Tab. 8, Continued

	HKT GLASSES														Avg.	St.D.
SiO_2	55.91	54.54	53.80	53.60	52.75	52.84	57.40	56.81	54.45	56.78	54.64	56.34	54.14	58.75	55.20	1.75
TiO_2	2.94	3.22	3.47	3.11	3.44	2.72	2.59	2.55	3.20	3.34	3.72	3.31	3.52	2.89	3.14	0.35
Al_2O_3	19.09	19.35	19.26	18.50	19.88	20.09	18.45	18.13	19.27	21.73	20.17	21.81	20.76	19.19	19.69	1.09
FeO_t	3.36	4.12	4.27	3.86	4.07	3.96	2.85	2.87	4.16	3.79	4.10	3.50	4.25	2.75	3.71	0.53
MnO	0.11	0.14	-	0.07	0.07	-	0.17	0.09	0.01	0.07	0.09	0.13	0.05	0.13	0.09	0.04
MgO	3.19	2.95	3.38	3.55	3.07	2.61	2.32	2.71	3.39	2.27	3.46	2.83	3.34	2.97	3.00	0.40
CaO	7.92	7.65	8.61	9.46	8.29	9.10	6.69	8.10	9.00	6.78	7.96	5.90	8.48	6.82	7.91	1.00
Na_2O	4.00	3.76	3.95	3.61	4.40	4.26	2.66	2.29	1.46	1.74	1.71	1.92	1.55	1.01	2.74	1.16
K_2O	2.48	2.36	2.37	2.16	2.43	2.44	4.59	4.24	1.66	2.05	1.93	1.99	1.86	2.61	2.51	0.82
Cr_2O_3	0.07	-	-	0.09	0.08	-	-	-	-	-	-	-	-	-	0.08	0.00
F	0.16	0.20	0.18	0.17	0.17	0.35	0.05	0.17	-	-	-	-	-	-	0.18	0.08
Sum	99.41	98.38	99.35	98.87	98.76	98.39	98.03	98.19	96.60	98.55	97.78	97.73	97.95	97.12	98.22	0.75
Na_2O+K_2O	6.48	6.12	6.32	5.77	6.83	6.69	7.25	6.52	3.12	3.79	3.64	3.91	3.41	3.62	5.25	1.49
Mg#	0.63	0.56	0.59	0.62	0.57	0.54	0.59	0.63	0.59	0.52	0.60	0.59	0.58	0.66	0.59	0.04
CIPW Norm, assuming $Fe_2O_3/FeO = 0.15$																
Q	6.55	6.57	3.80	5.87	1.53	1.30	5.03	5.48	8.85	12.47	7.78	12.87	7.18	13.45	7.05	3.69
C	0.00	0.00	0.00	0.00	0.00	0.00	0.00	0.00	0.00	1.98	0.00	3.56	0.00	0.00	0.40	1.01
or	23.61	22.23	23.32	21.33	26.01	25.14	15.71	13.50	18.67	20.33	20.15	21.39	19.20	16.01	20.47	3.50
ab	20.99	19.98	20.05	18.25	20.52	20.63	38.83	35.83	15.74	19.04	18.02	18.53	17.43	23.78	21.97	6.55
an	29.16	31.09	30.26	30.12	30.36	31.31	21.88	23.70	34.90	33.63	35.40	29.27	37.80	31.74	30.76	4.07
ne	0.00	0.00	0.00	0.00	0.00	0.00	0.00	0.00	0.00	0.00	0.00	0.00	0.00	0.00	0.00	0.00
di	7.65	5.43	9.79	9.87	8.43	10.98	8.85	12.89	7.68	0.00	3.19	0.00	3.35	1.48	6.40	4.02
hy	4.79	5.95	4.53	5.01	4.29	2.77	1.99	1.01	5.84	5.98	7.34	7.10	7.44	6.71	5.05	1.93
ol	0.00	0.00	0.00	0.00	0.00	0.00	0.00	0.00	0.00	0.00	0.00	0.00	0.00	0.00	0.00	0.00
mt	0.64	0.79	0.82	0.74	0.78	0.76	0.55	0.55	0.80	0.73	0.78	0.67	0.81	0.00	0.67	0.21
il	5.58	6.12	6.58	5.91	6.54	5.16	4.92	4.84	6.08	6.34	7.07	6.29	6.69	5.39	5.96	0.67

and olivine in some Zeppara Manna xenoliths. It was never found close to the pyrometamorphic glass. Texturally two types of phlogopite occur: 1) euhedral deformed stringers (0.5 mm long) in larger orthopyroxene crystals with equilibrium grain boundaries and 2) anhedral grains (~1 mm sized) along the contact with orthopyroxene and olivine and as veinlets cutting orthopyroxene (fig. 2*i-m*). Their Mg# (89.5-88.3) are roughly similar to coexisting olivine and pyroxenes, suggesting possible equilibrium with the other silicate phases. The composition (Table 7) falls in the field of phlogopite from sp-bearing mantle, being characterized by higher TiO_2 and Al_2O_3 as well as by lower SiO_2 respect to the garnet-peridotite mica from kimberlites.

Glass

Glass shows very different textural and chemical features (fig. 2*b,f,n*; Table 8). It occurs as: 1) «jacket glass» (Edgar *et al.*, 1989) along the contact between xenolith and host lava; 2) crosscutting veinlets; 3) interstitial pods and in melt pockets (pyrometamorphic glass) containing clinopyroxene and spinel relicts, together with microlites of olivine, clinopyroxene, spinel and rare feldspar. Only the pale yellow to reddish type glass, found in some Zeppara Manna samples, will be considered in this paper.

All the glasses are quartz-normative with 47.8 to 71.1 CIPW normative feldspars, and two of them are also corundum-normative. The glass composition (Table 8) shows SiO_2 ranging from 51.55 wt% to 58.75 wt%, high Al_2O_3 (18.0-23.1 wt%) and CaO (5.9-13.6 wt%), and variable TiO_2 (0.76-3.72 wt%), alkalies (0.94-7.25 wt%) and extremely variable Na_2O/K_2O. The most striking aspect is the bimodal distribution of K_2O and TiO_2. Indeed, glasses can be divided into: *(a)* low K_2O-TiO_2 (hereafter called LKT) type [average K_2O and TiO_2 = 0.07 wt% and 0.68 wt%, respectively, CaO (av. 11.36 wt%), MgO (av. 4.88 wt%) and FeO (av. 5.06 wt%)], and *(b)* high K_2O-TiO_2 (hereafter called HKT) type [average K_2O and TiO_2 = 2.51 wt% and 3.14 wt%, respectively, CaO (av. 7.91 wt%), MgO (av. 3.00 wt%) and FeO (3.71 wt%)]. The LKT glasses show a subalkaline character and basaltic andesite to andesite composition, whereas the HKT group is more alkali-rich and straddle the field of mugearite and trachyandesite (fig. 3).

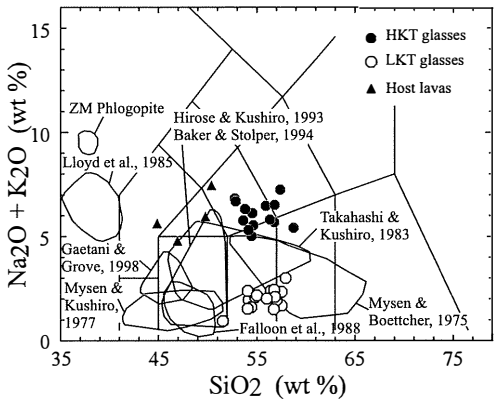

Fig. 3. – Total alkali silica diagram (Le Bas *et al.*, 1986). The fields indicates hydrous and anhydrous melting experiments on peridotitic to pyroxenitic sources. Filled triangles = host lavas; filled circles = Zeppara Manna HKT glasses; open circles = Zeppara Manna LKT glasses.

In terms of Mg# (assuming a Fe_2O_3/FeO ratio = 0.15) these glasses range from primitive liquid composition (Mg# = 0.71) to relatively evolved types (Mg# = 0.42), with the LKT glasses having generally higher values than the HKT ones. In fig. 4 the glasses are plotted in Harker-type diagrams. Some major elements such as MgO and CaO mimic a fractional crystallization path, with negative correlation with silica for both LKT and HKT, while Al_2O_3 and FeO do not show clear trends. The LKT glasses show an overall constant low TiO_2, K_2O and Na_2O/K_2O, while the HKT have a slightly negative correlation with TiO_2 and a broad positive correlation for Na_2O/K_2O ratio. The only substantial difference between LKT and HKT was noted for the Na_2O behaviour as incompatible element for LKT and more compatible for HKT.

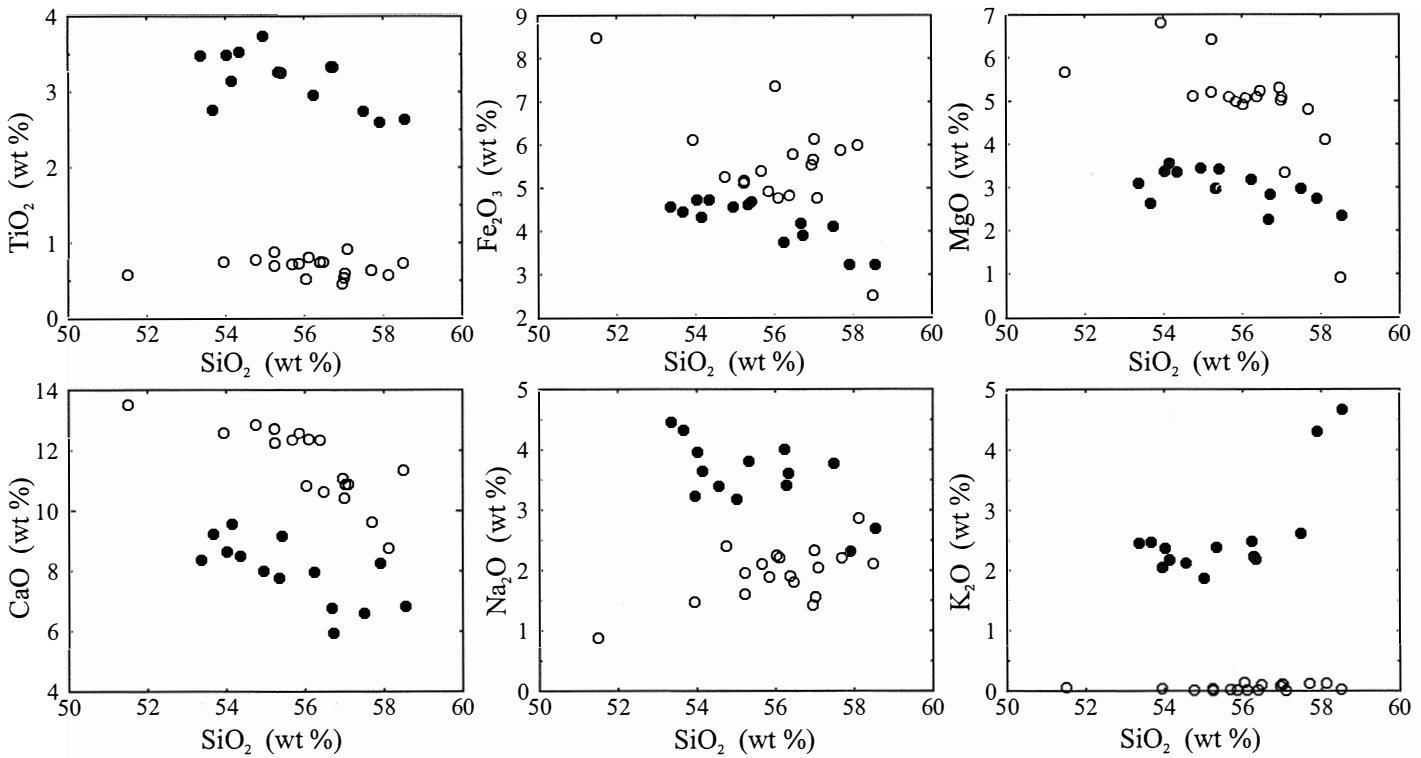

Fig. 4. – Major element diagrams versus SiO_2 for Zeppara Manna glasses. Filled circles = HKT glasses; open circles = LKT glasses.

GEOTHERMOBAROMETRY

Ten geothermometers and two geobarometers were used to constrain temperature and depth of equilibrium. Bearing in mind all the approximations of these algorithms due to analytical (Na and Fe^{3+} microprobe determination; Canil and O'Neill, 1996; Morgan and London, 1996), theoretical (non-ideal solution behavior, differences between simplified synthetic systems and natural paragenesis; Gutmann, 1986) and practical difficulties (lack of equilibrium in some mineral pairs due to different rates of diffusion, reaction and recrystallization; Fabries, 1979), all but one geothermometer gave broadly similar temperatures (Table 9; fig. 5).

All the models based on the pyroxene solvus gave broadly similar estimates. The *sp-ol* geothermometer of Fuji (1976) and Ballhaus *et*

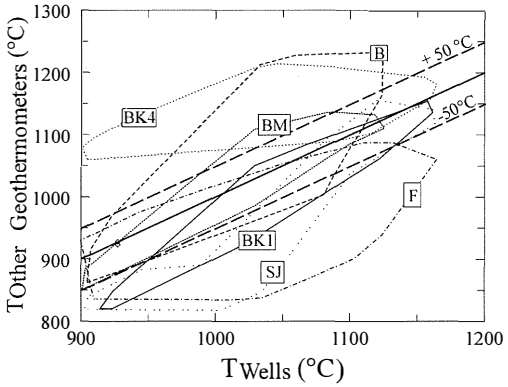

Fig. 5. – Geothermometric estimates utilising Well's (1977) method versus other geothermometers. (BM) = Bertrand and Mercier, 1986; (SJ) = Sen and Jones, 1989; (BK1) = Brey and Kohler, 1990 (Ca in orthopyroxene); (BK4) = Brey and Kohler, 1990(Ca and Fe in ortho- and clinopyroxene); (F) = Fuji, 1976; (B) = Ballhaus *et al.*, 1991 (based on a corrected and simplified version of the O'Neill and Wall (1987) olivine-spinel exchange geothermometer).

TABLE 9

Equilibrium temperature and pressure range for Zeppara Manna, Rio Girone and Pitzu Mannu mantle xenoliths. Geothermometers: B&M = Bertrand and Mercier (1986); B&K1-4 = Brey and Kohler (1990); S&J = Sen and Jones (1989); Ballh = Ballhaus et al. (1991); Wells = Wells (1977); Fujii = Fujii (1976); My&Bo = Mysen and Boettcher (1975). Geobarometer: Mercier = Mercier (1980). See text for explanations.

T (°C)	ZM-2			ZM-1			RG4b			MGL 22		
$B\&M_{(cpx\text{-}opx)}$	1100	1105	1101	1115	1123	1066	1108	1108	1107	925	913	913
$B\&K1_{(cpx\text{-}opx)}$	1050	1036	1051	1059	1079	1011	1047	1047	1065	847	833	833
$B\&K4_{(cpx\text{-}opx)}$	1199	1202	1202	1127	1132	1098	1206	1205	1205	1113	1102	1102
$S\&J_{(opx\text{-}cpx)}$	923	965	942	1036	1030	922	1030	1031	1045	878	850	860
$Ballh_{(ol\text{-}sp)}$	1133	1192	1153	987	1045	1120	1138	1020	1020	915	935	886
$Wells_{(cpx\text{-}opx)}$	1044	1050	1039	1083	1086	1041	1059	1059	1069	939	924	927
$Fujii_{(sp\text{-}opx\text{-}ol)}$	1038	1211	998	1029	957	848	943	986	989	988	829	923
$My\&Bo_{(cpx\text{-}opx)}$	1134	1060	1112	823	1041	928	1084	1087	1068	932	933	1003
Mean	*1078*	*1103*	*1075*	*1032*	*1062*	*1004*	*1077*	*1068*	*1071*	*942*	*915*	*931*
St. Dev.	*78*	*85*	*79*	*90*	*53*	*90*	*73*	*63*	*60*	*75*	*82*	*80*
P (kb)												
$Mercier_{(opx)}$	12.6	12.8	12.7	12.4	12.6	12.4	12.7	12.7	12.6	13.2	12.5	12.3

al (1991) gave the lowest and highest values, respectively. The bias between *sp-ol* and *cpx-opx* Wells' geothermometers could be explained by the difference in blocking temperatures of cations exchange reaction (Fabries, 1979). The data of Brey and Kohler (1990), based on partitioning of Na in ortho- and clinopyroxene, have not been reported in fig. 5 because of the very high temperatures obtained (up to 1500 °C). We related these high temperatures to analytical difficulties in microprobe alkalies determinations because of Na mobility under electron beam (Zinngrebe and Foley, 1995, Morgan and London, 1996). The Pitzu Mannu sample (MGL22) is characterized by average temperatures of ~950 °C, while the Zeppara Manna xenoliths (ZM1 and ZM2) and the Rio Girone sample (RG4b) show slightly higher average temperature estimates (~1050 °C).

Concerning the equilibration pressures, it must be noted the paucity of reliable geobarometers for xenoliths in the spinel facies (Gasparik, 1984). The *opx* geobarometer of Mercier (1980) gave a limited pressure range (12.4 to 13.2 kbar; Table 9), while the iterative *ol-cpx* geobarometer of Kohler and Brey (1990) gave much more scattered values (from ~10 to ~14 kbar), with very anomalous coexisting temperatures (up to 1500 °C). The anomalously higher temperature estimate and the scatter of barometric constraints of the *ol-cpx* geobarometer of Kohler and Brey (1990) are probably caused by the Ca content of the Gerrei mantle olivine, whose low concentration (all but one <0.16 wt%) is comparable with the lower detection limit of the electron microprobe (Lee *et al.*, 1996). With due precautions, these two geobarometers gave pressure of origin below the actual Moho discontinuity, localized in Sardinia at ~10 kbar (~35 km; Scarascia *et al.*, 1994); these pressure estimates are broadly in agreement with the geothermal gradient of 27-30°C/km deduced by Beccaluva *et al.* (1989) on the basis of CO_2-bearing inclusions in xenoliths from Pozzomaggiore.

Discussion

Origin of glass

It should be noted that glasses in mantle xenoliths are often associated with reactions which include destabilization of primary phases and/or crystallization of new phases. Basically, the glass in mantle xenoliths may have derived from: 1) infiltration of material external to the peridotitic assemblage which variably reacted with the preexisting phases, or 2) *in situ* partial melting of peridotitic phases due to decompression after incorporation within the host lava. In the first case the glass formation may have predated or be coeval with magmatic activity, while, in the second case it is necessarily contemporaneous with magmatic activity. In particular, the presence of glassy patches in mantle xenoliths has been variously attributed to:

1. *Reaction between infiltrating host lava and peridotite wall rock* (Hansteen *et al.*, 1991; Wulff-Pedersen *et al.*, 1996).

2. *Decompression melting of hydrous phases, like amphibole or phlogopite* (Frey and Green, 1974; Francis, 1976; Conticelli and Peccerillo, 1990; Chazot *et al.*, 1996; Yaxley *et al.*, 1997);

3. *Trapping of deep-seated material such as*:

3(a) H_2O/CO_2-rich alkaline silicate melts (Kuo and Essene, 1986; Edgar et al, 1989; Schiano and Clocchiatti, 1994; Zinngrebe and Foley, 1995; Kepezhinskas *et al.*, 1996; Sen *et al.*, 1996);

3(b) H_2O/CO_2-enriched fluids (Beccaluva *et al.*, 1989; Schiano *et al.*, 1992; Xu *et al.*, 1996);

3(c) carbonatite melts (Girod *et al.*, 1981; Jones *et al.*, 1983; Yaxley *et al.*, 1991; Rudnick *et al.*, 1993; Ionov *et al.*, 1993, 1994; Szabò *et al.*, 1995; Coltorti *et al.*, 1999);

4. *Partial melting product of «normal» mantle phases*: (Doukhan *et al.*, 1993; Raterron *et al.*, 1997; Draper and Green, 1997; Franz and Wirth, 1997).

1) *Glass as infiltration of host lava*

Infiltration of host magma is excluded in the case of the Gerrei glasses on the basis of

textural and chemical composition of the glass. The pale yellow to reddish glass is optically distinguishable from the brownish glass of magmatic origin, which sometimes cross-cuts the Gerrei xenoliths. The pyrometamorphic glass was found always in melt pockets within the xenolith, not linked with the host lava. Moreover, the glasses are quartz normative and show lower MgO and alkalies and higher SiO_2 than the ne-normative, relatively high MgO (up to 8.89 wt%) host lavas (Lustrino *et al.*, 1996).

2) *Glass as breakdown product of hydrous phases*

The presence of sporadic phlogopite may be indicative of past metasomatic events. The glasses could be thought of as breakdown products of this phase. In fig. 6*a* the ZM glass is plotted together with other mantle-glasses derived by incongruent melting of mica and/or amphibole. The composition of the glass derived by hydrous phases depends on the composition of the breakdown phase (Yaxley *et al.*, 1997). In fact, in fig. 6*a* two distinct arrays are shown: glasses favored by incongruent melting of phlogopite (e.g. Frey and Green, 1974; Conticelli and Peccerillo, 1990, Wilson and Downes, 1991) may have up to 8.5 wt% K_2O, and relatively low Na_2O, while glasses related with amphibole breakdown (e.g. Francis, 1976; Wilson and Downes, 1991; Chazot *et al.*, 1996) show the highest Na_2O (up to 9.6 wt %), with lower K_2O. The low Na_2O and, in particular, K_2O (K_2O down to 0.01 wt%) of the LKT glasses strongly argue against a derivation from phlogopite. Otherwise, the geochemistry of the HKT glasses (which show higher K_2O/CaO and TiO_2 than LKT) needs involvement of a relatively TiO_2- and K_2O-rich phase (see below).

A direct derivation of Zeppara Manna glasses from breakdown of phlogopite is also ruled out by their quartz-normative character (7.7-18.9 and 2.8-13.4 normative quartz of LKT and HKT glasses, respectively). The model recently proposed by Yaxley *et al.* (1997) invoking the reaction of orthopyroxene with a low SiO_2 melt (derived from the breakdown of hydrous phases), to produce olivine ± clinopyroxene plus a more SiO_2-rich residual liquid is similarly highly unlikely in the case of the Zeppara Manna glasses, because of the lack of reaction contacts between orthopyroxene and glass.

3(a)(b) *Glass as infiltration of siliceous melt or H_2O/CO_2-rich fluid*

Figure 6*b* shows a wider scatter of data relative to the glasses of fig 6*a*. The high variability of these glasses in terms of oxides (Na_2O 0.62-9.44 wt%; K_2O 0.79-10.43 wt%; CaO 0.13-14.58 wt%), associated with nepheline- to quartz-normative character, is linked to the variable nature of the metasomatic agents, to high (melt-fluid)/rock ratios (Chazot *et al.*, 1996) and to variable styles of evolution of the metasomatic processes.

The LKT glasses generally plot outside the fields of fig. 6*b*, implying different petrogenesis. The only substantial overlap is that with the Gees glasses of Zinngrebe and Foley (1995). These glasses (which reach up to 72 wt% SiO_2) were related to high-alumina calcalkaline melts formed by AFC-type processes between host basalts and peridotite wall rock, according to the model of Kelemen (1990). These assumptions are, nevertheless, in strong contrast with the petrography of the ZM xenoliths: the Gees glasses are always found rimming orthopyroxene porphyroclast relicts associated with aggregates of olivine and clinopyroxene microlites according to the reaction *opx+melt=ol+cpx+liquid* (Kelemen, 1990), while the Gerrei glass does not show any reaction with orthopyroxene or olivine, being associated almost exclusively to diopside and spinel.

3(c) *Glass as infiltration of carbonatitic melt*

The very low viscosity of carbonatite melt makes it an efficient metasomatic agent in incompatible trace element transport through the upper mantle (Rudnick *et al.*, 1993).

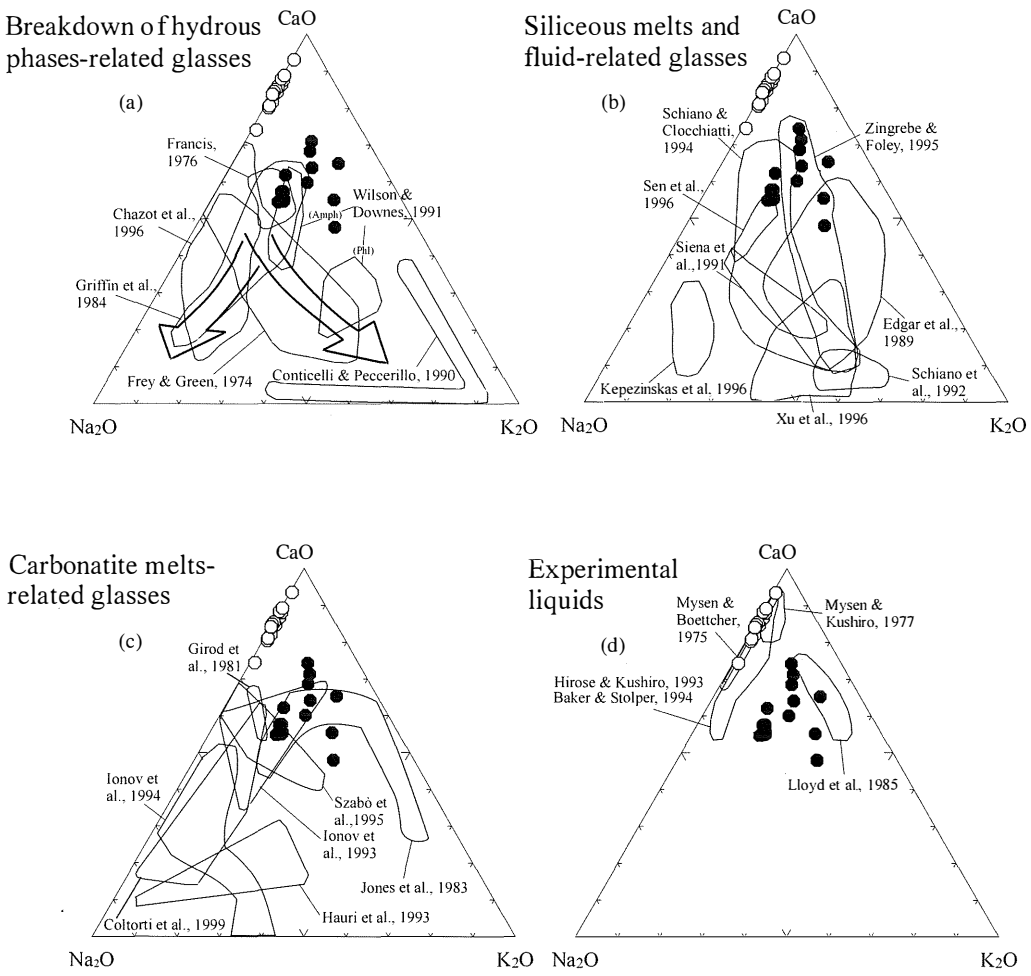

Fig. 6. – Na_2O-CaO-K_2O diagram for glasses in Zeppara Manna mantle xenoliths. Filled circles = HKT glasses; open circles = LKT glasses. *a)* = Glasses derived by breakdown of hydrous phases. The leftward arrow (toward Na_2O) indicate the pattern of amphibole-related glasses, while the right arrow (toward K_2O) imply a stronger involvement of phlogopite; *b)* = Glasses derived from siliceous melt and H_2O/CO_2 rich fluid metasomatism. The scatter of data is due to high (melt-fluid)/rock ratio: *c)* = Glasses derived from carbonatite metasomatism; *d)* = Liquids derived from melting experiments made on hydrous and anhydrous lherzolitic to pyroxenitic sources. See text for explanations.

In fig. 6*c* the Gerrei glasses, together with the field of glasses related to carbonatitic metasomatism, are shown. The idea of a carbonatitic metasomatism gained numerous preferences since the experimental studies of the last twenty years which evidenced the immiscibility between silicate and carbonatitic melts. The experimental study of Wallace and Green (1988) pointed out the occurrence of carbonatite (carbonate-rich) melts at upper mantle pressures and temperatures as very small melt fraction in equilibrium with pargasite lherzolite. These melts would be capable of enriching the peridotite in alkalies, LILE and LREE (Green and Wallace, 1988). The reaction with the peridotitic assemblage

would involve orthopyroxene to form jadeitic-rich clinopyroxene (Na_2O = 1.5-2 wt%) with high CaO/Al_2O_3 ratios (>6.5) according to the reaction: *enstatite + Ca-Na-rich melt = Na-diopside + forsterite ± chrome spinel + Ca-poor residual melt* (Green and Wallace, 1988; Yaxley *et al.*, 1991, 1997), causing overall whole rock enrichment in CaO, Na_2O, CaO/Al_2O_3 and Na_2O/Al_2O_3, and depletion in Al_2O_3 and TiO_2 with respect to the average subcontinental spinel lherzolite (McDonough, 1990). Petrographically, the whole rocks compositions would change from harzburgitic-lherzolitic types to wehrlitic or *cpx*-rich lherzolite. The extent of this transformation obviously depends on the disposal of reacting enstatite, and thus the more harzburgitic composition (orthopyroxene-rich), the more CaO-poor and SiO_2-rich the residual liquid.

The Gerrei mantle xenoliths were compared to the spinel peridotite xenoliths from Mt. Leura and Mt. Shadwell (western Victoria, Australia), strongly modified by carbonatite metasomatism (Green and Wallace, 1988; Yaxley *et al.*, 1991). As indicated above, with respect to the lithospheric mantle of McDonough (1990), the Victorian xenoliths show higher CaO/Al_2O_3 and Na_2O/Al_2O_3 whole rock ratios, whereas the Gerrei xenoliths resemble closer the McDonough's average lithospheric mantle (Table 1). Moreover, the experimentally crystallized clinopyroxenes of Wallace and Green (1988) show much higher CaO/Al_2O_3 and Na_2O/Al_2O_3 ratios (6.50-7.45 and 0.08-0.23, respectively) and much lower TiO_2 (0.27-0.73 wt%) compared to ZM diopsides included in glass (1.79-2.16, 0.04-0.06, and 4.79-5.32 wt%, respectively; Table 5). These evidences strongly argue against a carbonatitic precursor for the glass in the ZM xenoliths. Finally, the residual silicate melt, after reaction with orthopyroxene, would be Ca-poor, CaO being utilized to form diopsidic pyroxene. Also, the same glass would be K-rich, due to depletion in CaO which might enhance the K_2O and H_2O activity of the melt (Wallace and Green, 1988). On the other hand, the Gerrei glasses are Ca-rich and, especially the LKT-type, alkali-poor (Table 8). In summary, geochemical and petrographic evidences strongly argue against a carbonatitic melt-related origin of the Gerrei melt pockets.

Strong evidence against carbonatite metasomatism in the sub-continental mantle of this region come also from the Sr-Nd-Pb isotopic systematic of the Plio-Quaternary rocks of Sardinia (Lustrino, 1999). The carbonatite metasomatism-related modifications, would shift the isotopic compositions toward unradiogenic Sr and radiogenic Nd and Pb (e.g. Simonetti and Bell, 1994), while the host lavas of Zeppara Manna are characterized by unradiogenic Pb ($^{206}Pb/^{204}Pb$ = 17.87) and Nd ($^{143}Nd/^{144}Nd$ = 0.51258). These conclusions are in contrast with those obtained from mantle xenoliths and host lavas from Italy (e.g. Pantelleria Island (Civetta *et al.*, 1998), Mt. Etna (Tanguy *et al.*, 1997), Hyblean Mts. (Beccaluva *et al.*, 1998; Trua *et al.*, 1998)) and on CEVP rocks (e.g. Gees (Germany; Thibault *et al.*, 1992), Hungary (Szabò *et al.*, 1995), Massif Central (Ray Pic; Zangana *et al.*, 1997)). For these lavas and mantle xenoliths some petrographic, geochemical and isotopic characteristics have been related to carbonatitic-type metasomatism. Hence, this section underlines the differences of the subcontinental mantle sources of Sardinia with respect to those in other Mediterranean areas, already evidenced by major, trace element and isotopic geochemistry of the lavas (Lustrino *et al.*, 1996, 1998). This implies a different evolution of the mantle sources.

4) *Glass as primitive liquid*

Liquids derived from melting experiments on dry (Mysen and Kushiro, 1977; Takahashi and Kushiro, 1983; Hirose and Kushiro, 1993) and hydrous peridotite (Mysen and Boettcher, 1975; Mysen and Kushiro, 1977; Kushiro, 1990) and from a phlogopite-pyroxenite source (Lloyd *et al.*, 1985) are shown in fig 6*d*. These liquids show wide compositional range, with products of dry-melting having higher FeO,

MgO, CaO and alkalies, and lower SiO_2, TiO_2, Al_2O_3 than hydrous peridotites. However, it is worth noting the contrasting results often obtained by different researchers. For example, the content of SiO_2 in hydrous peridotite melting is thought to be higher (e.g. Hirose, 1997), broadly similar (Kushiro, 1990) or lower (Gaetani and Grove, 1998) compared to the partial melting products of anhydrous peridotite. Moreover, the SiO_2 of near-solidus melts, compared to higher temperature melts, was found to be higher (Raterron *et al.*, 1997; Gaetani and Grove, 1998), roughly the same (Takahashi and Kushiro, 1983; Baker and Stolper, 1994) or lower (Mysen and Kushiro, 1977). Lastly, the melt composition is thought to be independent (Hirose and Kushiro, 1993) or dependent (Robinson *et al.*, 1998) on bulk composition of the starting peridotite. The main discrepancies are related to the experimental technique adopted (Robinson *et al.*, 1998), to the artifact of normalization to a volatile-free basis the hydrous experimental melts (Gaetani and Grove, 1998), to the composition of the capsules (Draper and Green, 1997), to the uncertainties on thermocouples measurements (Baker and Stolper, 1994) and to different T-P-fO_2 conditions, quench problems, slow reaction rates in solids and interlaboratory calibration (Takahashi and Kushiro, 1983). All this means that the characteristics of partial melts of hydrous and anhydrous peridotite can be evidenced only in a general way and with some uncertainties. With these assumptions, it is possible to point out that the overall major element chemistry of the Zeppara Manna glasses (particularly the LKT) resembles the liquids generated from hydrous mantle (Mysen and Boettcher, 1975, Kushiro, 1990).

However, care has to be taken with the ZM glasses because of their strong geochemical and textural evidences of disequilibrium. First of all, both LKT- and HKT-type glasses show fractional crystallization paths (fig. 4), and thus they could represent residual liquids after crystallization of the microlites (olivine ± clinopyroxene ± spinel) from an original melt. Moreover, textural evidence of disequilibrium is the irregularly scalloped and spongy boundary of grains in contact with the glass (mainly clinopyroxene and spinel) and the irregular shape of the glass itself (fig. 2*f, n*). In particular, the shape of the glassy blebs indicates a formation shortly before the rise to the surface, because of the capillary action would have distributed the glass into triple junctions and along grain boundaries of primary phases (Yaxley *et al.*, 1997; Coltorti *et al.*, 1999).

The presence of spongy pyroxene, glassy blebs almost exclusively associated with diopside and spinel, and the high CaO and Al_2O_3 and low Na_2O and K_2O of the LKT glasses, could be evidence of non-modal partial melting of the peridotite, with diopside and spinel being the first phases to be consumed, as evidenced by several experimental studies (e.g. Baker and Stolper, 1994).

These observations agree with the experimental work of Doukhan *et al.* (1993) on early partial melting (EPM) in pyroxenes. The first amorphous material produced by EPM of diopside appeared several hundred degrees below the conventional solidus of clinopyroxene, and it is characterized by high SiO_2, Al_2O_3 and CaO coupled with low to very low MgO and alkalies. The same experiments on orthopyroxene did not produce glass below 1300 °C. However, more recent studies (Raterron *et al.*, 1997) detected early partial melting droplets also in olivine and orthopyroxene. These melts have been found both as intracrystalline droplets (0.1-0.5 μm) and as intergranular melt pockets with substantial chemical differences. In particular, the intergranular melt pockets consist of a matrix made up by 60-70 vol. % of crystallites of olivine plus 30-40 vol. % olivine and clinopyroxene relicts, plus 1-7 vol. % of quenched residual liquid. Thus, the composition of LKT-glasses share strong chemical and textural similarities with the EPM products experimentally obtained by Doukhan *et al.* (1993) and Raterron *et al.* (1997; Table 8).

Notably, the geothermometric estimates on the Sardinian xenoliths indicate subsolidus conditions, as compared to the melting temperature of peridotite at 10 kbar obtained by Baker and Stolper (1994). Indeed, the ~1240 °C (±10 °C) solidus temperature at 10 Kb experimentally measured on the Kilbourne Hole peridotite by Baker and Stolper (1994), is several hundreds degrees higher than the Well's two-pyroxenes equilibrium temperatures obtained on the Gerrei xenoliths (~950-1050°C). Moreover, the real solidus of the Gerrei xenoliths lies probably above the 1240°C solidus calculated on the Kilbourne Hole peridotite, as these Sardinian xenoliths are characterized by a slightly more restitic chemical character, and, therefore, by higher solidus temperature. Consequently, the presence of glass in the Zeppara Manna xenoliths does not indicate the intersection of mantle geotherm with the Sardinian lithospheric solidus. More probably, the cause of the incongruent melting of the ZM xenoliths could be due to the thermal gradient and/or the decompression occurred after the incorporation in the host lava (e.g. Franz and Wirth, 1997). Nevertheless, incongruent melting of diopside and spinel cannot explain the high K_2O (up to 4.6 wt%) and TiO_2 (up to 3.7 wt%) of HKT glasses and the high TiO_2 both of the enclosed diopside and spinel (up to 5.32 and 0.8 wt%, respectively). Considering that K_2O behaves as perfectly incompatible element during partial melting processes of clinopyroxene (±spinel ±olivine), and considering an undetectable amount of K_2O in these minerals (e.g. in the order of 0.001-0.01 wt%), an unreasonably low volume fraction of melt (f ~ 0.04-0.4 vol. %) would be necessary to obtain glasses with ~ 2.5 wt % of K_2O. These values are clearly too low and in disagreement with the relatively large area covered by the glassy patches.

The hypothesis of incongruent melting of clinopyroxene and spinel in mantle xenoliths was first postulated by Ionov *et al.* (1994) for Mongolian glasses. They related the glassy patches to *in situ* disequilibrium melting «involving largely clinopyroxene and spinel owing to reaction with migrating fluids». The anomalous Na_2O (up to 10.5 wt%) and K_2O (up to 4.7 wt%) was related by these authors to carbonatitic infiltration carrying high concentration of incompatible elements. As above stated, the possibility of a carbonatitic metasomatic process to explain the ZM glasses is, however, ruled out. The Gerrei glasses are petrographically, but not chemically, similar to the Mongolian xenoliths, (fig. 6*c*); therefore, different processes must be invoked.

PHLOGOPITE-GLASS RELATIONSHIPS

The need of a metasomatic agent to explain the composition of HKT glasses and related phases, focuses the attention on the high-Ti phlogopite, this phase being (as well as amphibole) the most reliable carrier of TiO_2 and K_2O (Wilkinson and Le Maitre, 1987; Luth, 1997).

The textural aspect of the mica indicates its presence in the peridotite wall rock before the xenolith incorporation by the host lava (e.g. Szabò *et al.* 1995) and thus not related with the host lavas: the (often strong) deformation of the ZM phlogopite is thought to be related to pressure release *en route* to the surface. The absence of relationships between host lavas and phlogopite from xenoliths is also evidenced by the different compositions of mica in equilibrium with host lavas and mantle phlogopite, the first being richer in SiO_2 (average 41 wt%), TiO_2 (av. 5.4 wt%), FeO (av. 6.1 wt%), MgO (av. 21.6 wt%) and K_2O (9.6 wt%), and poorer in Al_2O_3 (av. 11.4 wt%) and Mg# (av. 86.2; Lustrino, 1999) than the latter. On the other hand, the absence of devitrified patches, the shape of the glass and the presence of tiny quench microlites of plagioclase suggest more recent formation (just after the incorporation of the xenolith?) at lower pressure conditions (Ionov *et al.*, 1994; Yaxley *et al.*, 1997), e.g. within the *pl*-peridotite facies (<10 kbar; Takahashi and Kushiro, 1983).

The high TiO_2-K_2O phlogopite is likely to be

involved in the genesis at least of the HKT glasses. Regarding this system, Modreski and Boettcher (1973) experimentally found that the phlogopite-diopside system melts incongruently at 0.5-3 GPa to give olivine and liquid. Similar experiments at higher pressures (3-17 GPa; Luth, 1997) gave the same results, with formation of a SiO_2- and K_2O-rich liquid. The absence of this phase in the neighboring of the melt pockets and its occurrence only in distant portions (mainly within orthopyroxene or close to olivine) may be explained by the total exhaustion of small quantities of this phase during early partial melting events when in contact with eutectic-like minerals (e.g. along *cpx-sp-opx* or *cpx-sp-ol* triple junctions). Where included in orthopyroxene or olivine or at the contact with these grains, phlogopite did not participate to the melting. An increasing proportion of phlogopite (whose FeO is roughly similar to that of clinopyroxene) in the melt would not significantly alter the FeO content, while it can significantly modify TiO_2 and K_2O. Note that the LKT glasses plot along a near straight line between diopside and spinel for TiO_2, CaO, FeO and K_2O: this pattern (not shown) excludes the involvement of phlogopite in their genesis. The major element bimodality of the glasses (fig. 4) could indicate variable involvement of mica in the genesis of melt pockets, with HKT glasses being characterized by higher phlogopite component than the LKT glasses, whose chemical composition was buffered almost entirely by diopside and spinel.

Mass balance calculations

Mass balance calculations were carried out on HKT and LKT glasses in order to determine the reactions that may have related to the formation of these phases. Diopside may melt incongruently, giving a molten phase different from the starting material and the residual solid, according to the reaction: diopside (±spinel ±phlogopite) ⇒ olivine ±new spinel ±new clinopyroxene +Si-rich molten phase. The composition of the glass was calculated based on incongruent melting of a starting material made up mainly of diopside and spinel. The exact procedure is explained in Appendix.

HKT-Glasses – A starting mixture of ~94% clinopyroxene and 6% spinel was chosen. Considering the reaction of such mixture during a partial melting event involving crystallization of tiny microlites of diopside, spinel and olivine, plus consumption of about 5% phlogopite, a liquid, whose composition resembles the average of HKT glasses, was obtained. Euhedral microlites of diopside, olivine and spinel included in the glass were chosen as secondary phases, while relicts of diopside and spinel where used as starting material (primary phases). In this model an average of HKT glasses was used due to the relatively large variation in major element chemistry in the same thin section. This variability is probably due to variable contribution of the starting and crystallizing phases. The mass balance coefficients for the phases were obtained using the MS Excel® Solver macro routine, and a least squares residual <1 (~0.6) was obtained. The problem was set to obtain the minimum residual between an hypothetical starting material and a product made up by the average of the HKT glasses plus euhedral crystallites. Primary and secondary phases plus average HKT-glass are given in Table 10. The mass balance coefficients for reaction before hypothesized and successfully constrained are:

$$7.9\,Cpx_{(1)} + 0.5\,Sp_{(1)} + 0.7\,Phl \Rightarrow 3.8\,Cpx_{(2)} + 0.6\,Sp_{(2)} + 0.1\,Ol_{(2)} + 1.0\,Glass$$

where the subscripts (1) and (2) represent primary (reactant) and secondary (product) phases, respectively. This means that, in order to produce 6.9% of HKT glass, 54.3% of clinopyroxene, 3.3% spinel and 4.9% phlogopite are needed as starting material, and 25.9% of secondary clinopyroxene, 0.7% secondary olivine and 4.1% secondary spinel are needed as phases crystallizing from the molten phase. Note that: 1) Only small

TABLE 10

Mass balance calculations for the HKT-glasses (A) and LKT-glasses (B) of Zeppara Manna mantle xenoliths. Columns 1, 2 and 3 are, respectively, primary clinopyroxene, spinel and phlogopite which participate to mass balance calculations as starting material. Phlogopite analyses in column 3 are the average of 13 analyses; in the case of LKT glasses phlogopite is not involved. Column 4 represents the starting material and is, thus, the sum of columns 1 to 3 normalized to 100. Column 5 is the average of HKT (14 analyses) and LKT (16 analyses) glasses. Columns 6, 7 and 8 are the composition of, respectively, secondary olivine, clinopyroxene and spinel included in glasses of Zeppara Manna. The analyses in column 6 are the average of 10 euhedral olivine included in glass. Column 9 represents the whole composition of the products, and is, thus, the sum of columns 5 to 8 normalized to 100. Column 10 represents the difference between the composition of the starting material (column 4) and the products (glass + secondary phases, column 9). R^2 is the last squares residual of column 10. m.b.c. = mass balance coefficients as deduced from MS Excel® Solver macro set in order to obtain the minimum R^2. Symbol «%» represents the percentage of phases involved in the reaction: $Cpx_{(1)}+Sp_{(1)}\pm Phl \Rightarrow Cpx_{(2)}+Sp_{(2)}+Ol_{(2)}+Glass$.

(A)	1	2	3	4	5	6	7	8	9	10
	REAGENTS				PRODUCTS					R.-P.
	$Cpx_{(1)}$	$Sp_{(1)}$	Av. Phl	**St. Mat.**	Av. HKT	$Ol_{(2)}$	$Cpx_{(2)}$	$Sp_{(2)}$	**Gl+phases**	Difference
SiO_2	51.07	-	37.76	48.02	55.87	41.39	53.61	0.27	47.99	0.03
TiO_2	0.75	0.14	3.91	0.98	3.18	-	0.09	0.26	0.67	0.31
Al_2O_3	6.10	54.89	16.38	9.59	19.93	-	2.83	36.05	9.51	0.08
FeO	4.03	13.22	4.66	4.62	3.75	7.42	2.51	16.53	4.34	0.29
MgO	15.59	20.03	20.76	16.45	3.04	49.34	18.69	18.45	16.32	0.14
CaO	18.64	-	0.13	16.43	8.01	0.18	21.33	-	16.19	0.24
K_2O	-	-	8.91	0.71	2.63	-	-	-	0.48	0.23
Na_2O	1.53	-	0.71	1.40	3.50	-	0.26	-	0.82	0.58
										0.65 R^2
m.b.c.	7.92	0.48	0.72	9.11	1.00	0.09	3.77	0.59	5.46	
%	54.3	3.3	4.9	62.54	6.9	0.7	25.9	4.1	37.46	

(B)	1	2	3	4	5	6	7	8	9	10
	REAGENTS				PRODUCTS					R.-P.
	$Cpx_{(1)}$	$Sp_{(1)}$		**St. Mat.**	Av. LKT	$Ol_{(2)}$	$Cpx_{(2)}$	$Sp_{(2)}$	**Gl+phases**	Difference
SiO_2	51.07			47.75	56.44	41.39	53.61	0.27	47.94	-0.19
TiO_2	0.75	0.14		0.71	0.69	-	0.09	0.26	0.22	0.49
Al_2O_3	6.10	54.89		9.82	19.24	-	2.83	36.05	9.66	0.16
FeO	4.03	13.22		4.76	5.13	7.42	2.51	16.53	4.67	0.09
MgO	15.59	20.03		16.07	4.95	49.34	18.69	18.45	16.54	-0.47
CaO	18.64	-		17.42	11.52	0.18	21.33	-	16.64	0.79
K_2O	-	-		0.00	0.07	-	-	-	0.01	-0.01
Na_2O	1.53	-		1.43	1.97	-	0.26	-	0.56	0.87
										1.90 R^2
m.b.c.	6.94	0.56		7.50	1.00	0.09	3.48	0.57	5.14	
%	54.9	4.4		59.30	7.9	0.8	27.5	4.5	40.70	

amounts of phlogopite may account for the relatively high K_2O and TiO_2 of HKT glasses; 2) To obtain relatively SiO_2-rich glass (55.9 wt% as average) from a relatively SiO_2-poor starting material (48.2 wt%), a phase very poor in SiO_2 needs to be formed. Such a phase is likely to be spinel; 3) In agreement with petrographic observations, enstatite is not involved as a reactant.

In fig. 6*d* the HKT glasses plot within or close to the field of the experiments of Lloyd *et al.* (1985) on a mantle assemblage consisting of clinopyroxene, phlogopite and minor titanomagnetite. This may strengthen the idea of an involvement of phlogopite (plus clinopyroxene and spinel) in the genesis of the HKT glasses.

LKT-Glasses – The low K_2O and TiO_2 of the LKT glasses (ZM1) argue against mica contribution, and therefore a starting material composed only of clinopyroxene and spinel in the ratio 93:7 was chosen. The product clinopyroxene, spinel and olivine ratio is 84:14:2. Thus, the incongruent melting of diopside plus minor spinel may produce a relatively SiO_2-rich, alkali-poor molten phase plus secondary clinopyroxene, spinel and olivine crystallized from it. The olivine composition given in table 10 is the same average olivine used in the above calculations for the HKT glasses, there being no difference between olivine microlites from the two glasses. The mass balance coefficients found in order to minimize the square residual between the starting material (clinopyroxene+spinel) and the product (secondary clinopyroxene, olivine and spinel, plus the average LKT-glasses) are:

$$6.9\,Cpx_{(1)}+0.6\,Sp_{(1)} \Rightarrow$$
$$3.5\,Cpx_{(2)}+0.6\,Sp_{(2)}+0.1\,Ol_{(2)}+1.0\,Glass$$

This means that, in order to produce 7.9% glass, 54.9% of clinopyroxene and 4.4% spinel as starting material, and 27.5% of secondary clinopyroxene, 4.5% secondary spinel and 0.8% secondary olivine crystallizing from the molten phase are needed, respectively. The least square residual for this reaction is low (<2), in spite of the relatively strong variation of the major phases and the LKT glasses. Thus, the possibility to derive the glasses in the Zeppara Manna mantle xenoliths from the incongruent melting of diopside plus spinel (±phlogopite) appears to possible.

Many other mass balance coefficients may be obtained for the two postulated reactions, using slightly different compositions of primary and secondary phases. However, all other reactions requires the same general formula: $cpx + sp \pm phl \Rightarrow cpx + sp + ol + glass$.

In conclusion, the presence of glassy patches in the Zeppara Manna xenoliths are not consistent with a metasomatic processes, but only barometric and/or thermal disequilibrium of the phases. On the other hand, the presence of phlogopite laths require processes which metasomatized the Sardinian subcontinental mantle.

Origin of phlogopite

Phlogopite is not uncommon in the mantle from intraplate and active margin settings. Its origin can be related to fluids from the deep mantle (e.g. in the case of phlogopite in kimberlite breccia) or to crystallization from alkali-rich fluids released from subducted slab (e.g. Modreski and Boettcher, 1973; Sudo and Tatsumi, 1990; Schiano *et al.*, 1992).

As noted above, phlogopite is thought to be the carrier of K_2O, TiO_2 and H_2O in the Earth's upper mantle, but it is also a possible major Pb reservoir, due to its high Pb concentration (> 20 ppm; Rosenbaum, 1993; Ionov *et al.*, 1997). The metasomatic agent from which phlogopite crystallized, being relatively Pb-rich, would have had low U/Pb and thus low μ. Thus, the origin of phlogopite laths in the ZM xenoliths and the unradiogenic-Pb character of the ZM host lavas and of the vast majority of the Plio-Pleistocene volcanic rocks of Sardinia (Lustrino, 1999) could have a unique precursor.

However, this hypothesis is hard to reconcile with the relatively low $^{87}Sr/^{86}Sr$ of the host rocks (0.7045 ± 1). In fact, the fluid from which phlogopite crystallized might be characterized by low U/Pb and high Rb/Sr ratios (Ionov *et al.*, 1997), while the modifications of the lithospheric sources of the Plio-Pleistocene volcanic rocks of Sardinia are characterized by low U/Pb, but also by a relatively low Rb/Sr (in order to prevent sensible radiogenic growth of the $^{87}Sr/^{86}Sr$ ratio). In conclusion, the causes of the isotopic character of the Sardinian rocks and those responsible for the crystallization of phlogopite in the Sardinian lithospheric mantle seem to be different. The presence of phlogopite in mantle xenoliths from the Nògrad-Gomor Volcanic Field (Carpathian-Pannonian Basin) have been related to the previous subduction-related magmatic cycle which enriched the subcontinental source in LILE (Szabò and Taylor, 1994). A similar origin for phlogopite in the Zeppara Manna xenoliths can be only speculated. On the other hand, the high Ba, Ba/Nb and K_2O of some host lavas from the Giara di Gesturi (Gerrei), thought to be related to metasomatic modifications that occurred during the previous Hercynian Orogeny (Lustrino *et al.*, 1996; Lustrino, 1999), may be considered the most plausible effects of such processes.

CONCLUSIONS

Lherzolite mantle xenoliths from central-southern Sardinia contain glassy blebs and sporadic phlogopite. The glassy matrix (which contains crystallites of olivine, clinopyroxene and spinel) is chemically divided into two types: LKT-type (with low TiO_2 and K_2O) and HKT-type (with high TiO_2 and K_2O). These glassy blebs occur associated with clinopyroxene and spinel relicts and do not show reaction contacts with olivine and orthopyroxene. Incongruent melting of clinopyroxene and spinel, as consequence of rise in temperature and drop of pressure after the incorporation within the host lava, could be responsible for high CaO and Al_2O_3 of both the glasses, respectively. The relatively high SiO_2 of the glasses (higher than SiO_2 of diopside) was related to the incongruent melting of clinopyroxene and spinel, with crystallization of a virtually SiO_2-free phase (new spinel) according to the reaction $cpx + sp \pm phl \Rightarrow ol + sp + cpx$ + glass. The involvement of phlogopite in the starting material is needed to explain the relatively high TiO_2 and K_2O of some glasses (HKT-type) whereas the LKT-type glasses are almost entirely buffered only by clinopyroxene and spinel.

An origin of phlogopite before the incorporation of the xenoliths within the host lava is postulated. This origin could be related to metasomatic influx of K-rich subduction-related fluids from deeper sources.

APPENDIX

To calculate the mass balance equations, the MS Excel® Solver macro routine was used in the following way: a couple of primary clinopyroxene and spinel analyses for LKT-glass modelization, and clinopyroxene, spinel and phlogopite analyses for HKT-glass modelization were chosen as reactant material. These assemblages were hypothesized to melt incongruently to give a molten phase plus secondary clinopyroxene, spinel and olivine. The composition of these secondary phases was added to the average composition of the LKT and HKT glasses to obtain the overall product. If the hypothesis of incongruent melting of the starting material is correct, and if the system is closed, the difference between reactant and the overall product must be equal to zero. The routine was imposed to iteratively obtain the least square residual between the starting material (clinopyroxene + spinel ± phlogopite) and the products of melting (glass + secondary phases) only changing the mass balance coefficient (m.b.c.) of all the terms (except the glass, which was fixed to 1.00). The percentage of the involved phases were calculated normalizing to 100 the m.b.a..

ANALYTICAL TECHNIQUES

Whole rock major and trace elements analyses were performed at University of Naples with a Philips PW1400 XRF spectrometer, Rh and W

anodes, at the Dipartimento di Scienze della Terra, utilizing pressed powder pellets, according to the method of Franzini *et al.* (1975) and Leoni and Saitta (1976). Loss on ignition (LOI), Na_2O and MgO, have been analyzed with standard gravimetric and atomic absorption spectroscopy (AAS), respectively. Electron microprobe analyses have been performed at CNR-CSGIC, Rome, utilizing a CAMECA SX-50 operating at 15kV and 15 nA. The data were reduced according to the PAP correction method. The electron beam used for silicates and spinel (variable from ~1 to 5 μm) was defocused to 10 μm when analyzing the glasses in order to prevent alkali loss.

ACKNOWLEDGEMENTS

Michele Lustrino thanks E. Mascia for database collection. G. Cavarretta and M. Serracino are thanked for their usual help during microprobe analyses. Thanks also to P. Brotzu for comments on an early version of the manuscript, and to A. Cundari for checking our English and for helpful discussions. Official review of M. Coltorti and G. Sen greatly improved this paper. This work was supported by MURST grant (60%; V.M.).

REFERENCES

AURISICCHIO C. and SCRIBANO V. (1987) — *Some ultramafic xenoliths from Etna.* Rend. Soc. It. Min. Petr., **42**, 219-224.

BAKER M.B. and STOLPER E.M. (1994) — *Determining the composition of high-presssure melts using diamond aggregates.* Geochim. Cosmochim. Acta, **13**, 2811-2827.

BALLHAUS C., BERRY R.F. and GREEN D.H. (1991) — *High pressure experimental calibration of the olivine-orthopyroxene-spinel oxygen geobarometer: implications for the oxidation state of the upper mantle.* Contrib. Mineral. Petrol., **107**, 27-40.

BANDA E., EGGER A., DEMARTIN M., MAISTRELLO M. and ANSORGE J. (1985) — *Crustal structure under Sardinia*: Proc. 2nd EGT Workshop - the southern segment. European Science Foundation, 201-203.

BECCALUVA L., CIVETTA L., MACCIOTTA G. and RICCI C.A. (1985) — *Geochronology in Sardinia: results and problems.* Rend. Soc. It. Min. Petr., **40**, 57-72.

BECCALUVA L., SIENA F., COLTORTI M., DI GRANDE A., LO GIUDICE A., MACCIOTTA G., TASSINARI R. and VACCARO C. (1998) — *Nephelinitic to tholeiitic magma generation in a transtensional tectonic setting: an integrated model for the Iblean volcanism, Sicily.* J. Petrol., **39**, 1547-1576.

BECCALUVA L., MACCIOTTA, G., SIENA, F. and ZEDA, O. (1989) — *Harzburgite-lherzolite xenoliths and clinopyroxene megacrysts of alkaline basic lavas from Sardinia. (Italy).* Chem. Geol., **77**, 331-345.

BREY G.P. and KOHLER T.P. (1990) — *Geothermobarometry in four-phase lherzolites II. New thermobarometers, and practical assesment of existing thermobarometers.* J. Petrol., **31**, 1353-1378.

CANIL D. and O'NEILL H.ST.C. (1996) — *Distribution of ferric iron in some upper-mantle assemblages.* J. Petrol., **37**, 609-635.

CHAZOT G., MENZIES M. and HARTE B. (1996) — *Silicate glasses in spinel lherzolites from Yemen: origin and chemical composition.* Chem. Geol., **134**, 159-179.

CIVETTA L., D'ANTONIO M., ORSI, G. and TILTON, G.R. (1998) — *The geochemistry of volcanic rocks from Pantelleria island, Sicily channel: petrogenesis and characteristics of the mantle source region.* J. Petrol., **39**, 1453-1491.

COLTORTI M., BONADIMAN C., HINTON R.W., SIENA F. and UPTON, B.G.J. (1999) — *Carbonatite metasomatism of the oceanic upper mantle: evidence from clinopyroxenes and glasses in ultramafic xenoliths of Grande Comore, Indian Ocean.* J. Petrol., in press.

CONTICELLI S. and PECCERILLO A. (1990) — *Petrological significance of high-pressure ultramafic xenoliths from ultrapotassic rocks of central Italy.* Lithos, **24**, 305-322.

DOUKHAN N., DOUKHAN J.C., INGRIN J., JAOUL O. and RATERRON P. (1993) — *Early partial melting in pyroxenes.* Am. Mineral., **78**, 1246-1256.

DRAPER D.S. and GREEN T.H. (1997) — *P-T phase relations of silicic, alkaline, aluminous mantle-xenolith glasses under anhydrous and C-O-H-fluid-saturated conditions.* J. Petrol., **38**, 1187-1224.

DROOP G.T.R. (1987) - *A general equation for estimating Fe^{3+} concentrations in ferromagnesian silicates and oxides from microprobe analyses, using stoichiometric criteria.* Min. Mag., **51**, 431-435.

EDGAR A.D., LLOYD F.E., FORSYTH D.M. and BARNETT, R.L. (1989) — *Origin of glass in upper mantle xenoliths from the Quaternary volcanics of Gees, West Eifel, Germany.* Contrib. Mineral. Petrol., **103**, 277-286.

FABRIES J. (1979) — *Spinel-olivine geothermometry in peridotites from ultramafic complexes.* Contrib. Mineral. Petrol., **69**, 329-336.

FRANCIS D.M. (1976) — *The origin of amphibole in lherzolite xenoliths from Nunivak island, Alaska.* J. Petrol., **17**, 357-378.

FRANZ L. and WIRTH R. (1997) — *Thin intergranular melt films and melt pockets in spinel peridotite xenoliths from the Rhon area (Germany): early stage of melt generation by grain boundary melting.* Contrib. Mineral. Petrol., **129**, 268-283.

FRANZINI M., LEONI L. and SAITTA M. (1975) — *Revisione di una metodologia analitica per fluorescenza-X, basata sulla correzione completa degli effetti di matrice.* Rend. Soc. It. Miner. Petrol., **31**, 365-378.

FREY F.A. and GREEN D.H. (1974) — *The mineralogy, geochemistry and origin of lherzolite inclusions in Victorian basanites.* Geochim. Cosmochim. Acta, **38**, 1023-1059.

FREY F.A. and PRINZ M. (1978) — *Ultramafic inclusions from San Carlos, Arizona: petrologic and geochemical data bearing on their petrogenesis.* Earth Planet. Sci. Lett., **38**, 129-176.

FUJI T. (1976) — *Solubility of Al_2O_3 in enstatite coexisting with forsterite and spinel.* Carnegie Inst. Washington D.C., **75**, 566-571

GAETANI G.A. and GROVE T.L. (1998) — *The influence of water on melting of mantle peridotite.* Contrib. Mineral. Petrol., **131**, 323-346.

GASPARIK T. (1984) – *Two-pyroxene thermobarometry with new experimental data in the system CaO-MgO-Al_2O_3-SiO_2.* Contrib. Mineral. Petrol., **87**, 87-97.

GIROD M., DAUTRIA J.M., DE GIOVANNI R. (1981) — *A first insight into the constitution of the upper mantle under the Hoggar area (southern Algeria): the lherzolite xenoliths in the alkali basalts.* Contrib. Mineral. Petrol., **77**, 66-73.

GUTMAN J.T. (1986) — *Origin of four and five phase ultramafic xenoliths from Sonora, Mesico.* Am. Mineral., **71,** 1076-1084.

GREEN D.H. and WALLACE M.E. (1988) — *Mantle metasomatism by ephemeral carbonatite melts.* Nature, **336**, 459-461.

HANSTEEN T.H., ANDERSEN T., NEUMANN E.R. and JELSMA H. (1991) — *Fluid and silicate glass inclusions in ultramafic and mafic xenoliths from Hierro, Canary islands: implications for mantle metasomatism.* Contrib. Mineral. Petrol., **107**, 242-254.

HIROSE K. (1997) — *Melting experiments on lherzolite KLB-1 under hydrous conditions and the generation of high-magnesian andesitic melts* Geology, **25**, 42-44.

HIROSE K. and KUSHIRO I. (1993) — *Partial melting of dry peridotites at high pressures: determination of compositions of melts segregated from peridotite using aggregates of diamond.* Earth Planet. Sci. Lett., **114**, 477-489.

IONOV D.A., DUPUY C., O'REILLY S.Y., KOPYLOVA M.G., GENSHAFT Y.S. (1993) — *Carbonated peridotite xenoliths from Spitsbergen: implications for trace element signature of mantle carbonate metasomatism.* Earth Planet. Sci. Lett., **119**, 283-297.

IONOV D.A., HOFMANN A.W. and SHIMIZU N. (1994) — *Metasomatism-induced melting in mantle xenoliths from Mongolia.* J. Petrol., **35**, 753-78.

IONOV D.A., GRIFFIN W.L., O'REILLY S.Y. (1997) — *Volatile-bearing minerals and lithophile trace elements in the upper mantle.* Chem Geol., **141**, 153-184.

JAGOUTZ E., PALME H., BADDENHAUSEN H., BLUM K., CENDALES M., DREIBUS G., SPETTEL B., LORENZ V. and WANKE H. (1979) — *The abundances of major, minor and trace elements in the Earth's Mantle as derived from primitive ultramafic nodules.* Proc. Lunar. Planet. Sci. Conf., 10th., 2031-2050.

JONES A.P., SMITH J.V. and DAWSON J.B. (1983) — *Glasses in mantle xenoliths from Olmani, Tanzania.* J. Geol., **91**, 167-178.

KELEMEN P.B. (1990) — *Reaction between ultramafic rock and fractionating basaltic magma I. phase relations, the origin of calc-alkaline magma series, and the formation of discordant dunite.* J. Petrol., **31**, 51-98.

KEPEZHINSKAS P.K., DEFANT M.J. and DRUMMOND M.S., (1996) — *Na metasomatism in the island-arc mantle by slab melt-peridotite interaction: evidence from mantle xenoliths in the north Kamchatka Arc.* «J. Petrol.», **36**, 1505-1527.

KOHLER T.P., BREY G.P. (1990) — *Calcium exchange between olivine and clinopyroxene calibrated al a geothermobarometer for natural peridotites from 2 to 60 kb with applications.* Geochim. Cosmochim. Acta, **54**, 2375-2388.

KUO L.C. and ESSENE E.J. (1986) — *Petrology of spinel harzburgite xenoliths from the Kishb plateau, Saudi Arabia.* Contrib. Mineral. Petrol., **93,** 335-346.

KUSHIRO I. (1990) — *Partial melting of mantle wedge and evolution of island arc crust.* J. Geophys. Res., **95**, 15929-15939.

LE BAS M.J., LE MAITRE R.W., STRECKEISEN A. and ZANETTIN, B. (1986) — *A chemical classification of volcanic rocks based on the total alkali-silica diagram.* J. Petrol., **27**, 745-750.

LEE D.C., HALLIDAY A.N., DAVIES G.R., ESSENE E.J., FITTON J.G. and TEMDJIM R. (1996) — *Melt enrichment of shallow depleted mantle: a detailed petrological, trace element and isotopic study of*

mantle derived xenoliths and megacrysts from the Cameroon line. J. Petrol., **37**, 415-441.

LEONI L. and SAITTA M. (1976) — *X-Ray fluorescence analysis of 29 trace elements in rock and mineral standards.* Rend. Soc. It. Mineral. Petrol., **32**, 497-510.

LLOYD F.E., ARIMA M. and EDGAR A.D. (1985) — *Partial melting of a phlogopite-clinopyroxenite nodule from south-west Uganda: an experimental study bearing on the origin of highly potassic continental rift volcanics.* Contrib. Mineral. Petrol., **91**, 321-329.

LUSTRINO M. (1999) — *Petrogenesis of Plio-Quaternary volcanic rocks from Sardinia: possible implications on the evolution of the European subcontinental mantle*, 188 pp. Ph.D. thesis, University of Naples.

LUSTRINO M., MELLUSO L., MORRA V. and SECCHI, F. (1996) — *Petrology of Plio-Quaternary volcanic rocks from central Sardinia.* «Per. Mineral.», **65**, 275-287.

LUSTRINO M., MELLUSO L., and MORRA V. (1998) — *Trace elements and Sr-Nd-Pb isotope geochemistry of Plio-Quaternary volcanic rocks of Sardinia (Italy).* IAVCEI congress, Cape Town, abstract, 37.

LUTH R.W. (1997) — *Experimental study of the system phlogopite-diopside from 3.5 to 17 GPa.* Am. Mineral., **82**, 1198-1209.

MCDONOUGH W.F. (1990) — *Constraints on the composition of the continental lithospheric mantle.* Earth Planet. Sci. Lett., **101**, 1-18.

MENZIES M.A. and HAWKESWORTH C.J. (eds) (1987) — *Mantle metasomatism.* Academic Press Geology series, 472 pp.

MERCIER J.C. (1980) — *Single-pyroxene thermobarometry.* Tectonophysics, **70**, 1-37.

MERCIER J.C. and NICOLAS A. (1975) — *Textures and fabrics of upper mantle peridotites as illustrated by xenoliths from basalts.* J. Petrol., **16**, 454-487.

MODRESKI P.J. and BOETTCHER A.L. (1973) — *Phase relationship of phlogopite in the system K_2O-MgO-CaO-Al_2O_3-SiO_2-H_2O to 35 kilobars: a better model for micas in the interior of Earth.* Am. J. Sci., **273**, 385-414.

MORGAN G.B. VI, LONDON D. (1996) — *Optimizing the electron microprobe analysis of hydrous alkali aluminosilicate glasses.* Am. Mineral. **81**, 1176-1185.

MORRA V., SECCHI F. and ASSORGIA A. (1994) — *Petrogenetic significance of peralkaline rocks from Cenozoic calcalkaline volcanism from SW Sardinia, Italy.* Chem. Geol., **118**, 109-142.

MORRA V., SECCHI F., MELLUSO L. and FRANCIOSI L. (1997) — *High-Mg subduction-related Tertiary basalts in Sardinia, Italy.* Lithos, **40**, 69-91.

MYSEN B.O. and BOETTCHER A.L. (1975) — *Melting of a hydrous mantle: II. Geochemistry of crystalsand liquids formed by anatexis of mantle peridotite at high pressures and temperatures as a function of controlled activities of water, hydrogen, and carbon dioxide.* J. Petrol., **16**, 549-593.

MYSEN B.O. and KUSHIRO I. (1977) — *Compositional variations of coexisting phases with degree of melting of peridotite in the upper mantle.* Am. Mineral., **62**, 843-865.

PIKE J.E.N. and SCHWARZMAN E.C. (1977) — *Classification of textures in ultramafic xenoliths.* J. Geol., **85**, 49-61.

RATERRON P., BUSSOD G.Y., DOUKHAN N. and DOUKHAN J.C. (1997) — *Early partial melting in the upper mantle: an A.E.M. study of a lherzolite experimentally annealed at hypersolidus conditions.* Tectonophysics, **279**, 79-91

ROBINSON J.A.C., WOOD B.J. and BLUNDY J.D. (1998) — *The beginning of melting of fertile and depleted peridotite.* Earth Planet. Sci. Lett., **155**, 97-111.

ROSENBAUM J.M. (1993) — *Mantle phlogopite: a significant lead repository?* Chem. Geol., **106**, 475-483.

ROSENBAUM J.M., WILSON M. and DOWNES H. (1997) — *Multiple enrichment of the Carpathian-Pannonian mantle: Pb-Sr-Nd isotope and trace element constraints.* J. Geophys. Res., **102**, 14947-14961.

RUDNICK R.L., MCDONOUGH W.F. and CHAPPELL B.W. (1993) — *Carbonatite metasomatism in the northern Tanzaian mantle: petrographic and geochemical characteristics.* Earth Planet. Sci. Lett., **114**, 463-475.

SCARASCIA S., LOZEJ A., CASSINIS R. (1994) — *Crustal structures of the Ligurian, Tyrrhenian and Ionian seas and adjecent onshore areas interpreted from wide-angle seismic profiles.* Boll. Geof. Teor. Appl., **36**, 5-19.

SCHIANO P., and CLOCCHIATTI R. (1994) — *Worldwide occurrence of silica-rich melts in sub-continental and sub-oceanic mantle minerals.* Nature, **368**, 621-624.

SCHIANO P., CLOCCHIATTI R. and JORON J.L. (1992) — *Melt and fluid inclusions in basalts and xenoliths from Tahaa island, Society archipelago: evidence for a metasomatized upper mantle.* Earth Planet. Sci. Lett., **111**, 69-82.

SEN G., MACFARLANE A. and SRIMAL N. (1996) — *Significance of rare hydrous alkaline melts in Hawaiian xenoliths.* Contrib. Mineral. Petrol., **122**, 415-427.

SIENA F. and COLTORTI M. (1993) — *Thermobarometric evolution and metasomatic processes of upper mantle in different tectonic settings: evidence from spinel peridotite xenoliths.* Eur. J. Mineral., **5**, 1073-1090.

SIMONETTI A. and BELL K. (1994) — *Isotopic and geochemical investigation of the Chilwa island carbonatite complex, Malawi: evidence for a depleted mantle source region, liquid immiscibility, and open-system behaviour.* J. Petrol., **35**, 1597-1621.

SUDO A. and TATSUMI Y. (1990) — *Phlogopite and K-amphibole in the upper mantle: implication for magma genesis in subduction zones.* Geophys. Res. Lett., **17**, 29-32.

SZABO' Cs. and TAYLOR L.A. (1994) — *Mantle petrology and geochemistry beneath Nògràd-Gomor volcanic field, Carpathian-Pannonian region.* Intern. Geol. Rev., **36**, 328-358.

SZABO' Cs., VASELLI O., VANNUCCI R., BOTTAZZI P., OTTOLINI L., CORADOSSI N. and KUBOVICS, I. (1995) — *Ultramafic xenoliths from the Little Hungarian Plain (western Hungary): a petrologic and geochemical study.* Acta Vulcanol., **7**, 249-263.

TAKAHASHI E. and KUSHIRO I. (1983) — *Melting of a dry peridotite at high pressures and basalts magma genesis.* Am. Mineral., **68**, 859-879.

TANGUY J.C. CONDOMINES M. and KIEFFER G. (1997) — *Evolution of the Mount Etna magma: constraints on the present feeding system and eruptive mechanism.* J. Volc. Geotherm. Res., **75**, 221-250.

THIBAULT Y., EDGAR A.D. and LLOYD F.E. (1992) — *Experimental investigation of melts from a carbonated phlogopite lherzolite: implications for metasomatism in the continental lithosphere.* Am. Mineral., **77**, 784-794.

TONARINI S., ARMIENTI P., D'ORAZIO M., INNOCENTI F. and SCRIBANO V. (1996) — *Geochemical features of eastern Sicily lithosphere as probed by Hyblean xenoliths and lavas.* Eur. J. Mineral., **8**, 1153-1173.

TRUA T., ESPERANÇA S. and MAZUOLI, R. (1998) — *The evolution of the lithospheric mantle along the N. African plate: geochemical and isotopic evidence from the tholeiitic and alkaline volcanic rocks of the Hyblean plateau, Italy.* Contrib. Mineral. Petrol., **131**, 307-322.

WALLACE M.E. and GREEN D.H. (1988) — *An experimental determination of primary carbonatite magma composition.* Nature, **335**, 343-345.

WELLS P.R.A. (1977) — *Pyroxene thermometry in simple and complex systems.* Contrib. Mineral. Petrol., **62**, 165-185.

WERLING F. and ALTHERR R. (1997) — *Thermal evolution of the lithosphere beneath the French Massif Central as deduced from geothermobarometry on mantle xenoliths.* Tectonophysics, **275**, 119-141.

WILKINSON J.F.G. and LE MAITRE R.W. (1987) — *Upper mantle amphiboles and micas and TiO_2, K_2O and P_2O_5 abundances and 100 $Mg/(Mg+Fe^{2+})$ ratios of common basalts and andesites: implications for modal mantle metasomatism and undepleted mantle compositions.* J. Petrol., **28**, 37-73.

WILSON M., DOWNES H. (1991) — *Tertiary-Quaternary extension-related alkaline magmatism in western and central Europe.* J. Petrol., **32**, 811-849.

WULFF-PEDERSEN E., NEUMANN E.R. and JENSEN B.B. (1996) — *The upper mantle under La Palma, Canary islands: formation of Si-K-Na-rich melt and its importance as a metasomatic agent.* Contrib. Mineral. Petrol., **125**, 113-139.

XU U., MERCIER J.C.C., MENZIES M.A., ROSS J.V., HARTE B., LIN C. and SHI L. (1996) — *K-rich glass-bearing wehrlite xenoliths from Yitong, northeastern China: petrological and chemical evidence for mantle metasomatism.* Contrib. Mineral. Petrol., **125**, 406-420.

YAXLEY G.M., CRAWFORD A.J. and GREEN D.H. (1991) — *Evidence for carbonatite metasomatism in spinel peridotite xenoliths from western Victoria, Australia.* Earth Planet. Sci. Lett., **107**, 305-317.

YAXLEY G.M., KAMENETSKY V., GREEN D.H. and FALLOON T.J. (1997) — *Glasses in mantle xenoliths from western Victoria, Australia, and their relevance to mantle processes.* Earth Planet. Sci. Lett., **148**, 433-446.

ZANGANA N.A., DOWNES H., THIRLWALL M.F. and HEGNER E. (1997) — *Relationship between deformation, equilibration temperatures, REE and radiogenic isotopes in mantle xenoliths (Ray Pic, Massif Central, France): an example of Plume-Lithosphere interaction?* Contrib. Mineral. Petrol., **127**, 187-203.

ZINNGREBE E. and FOLEY S.F. (1995) — *Metasomatism in mantle xenoliths from Gees, West Eifel, Germany: evidence for the genesis of calc-alkaline glasses and metasomatic Ca-enrichment.* Contrib. Mineral. Petrol., **122**, 79-96.